CHAPTER 11

ENABLING FORMULATIONS

> "If an elderly but distinguished scientist says that something is possible he is almost certainly right, but if he says that it is impossible he is very probably wrong."
>
> —Arthur C. Clarke

Biopharmaceutical modeling is expected to be a useful tool for design and selection of an enabling formulation. The suitability of an enabling formulation is different for each drug. A trial and error approach has been undertaken to find a suitable enabling formulation. However, there is a high demand to improve the efficiency of drug discovery and development. By understanding the rate-limiting process, rational design and selection of an enabling formulation would become possible. In this chapter, each enabling technique is reviewed from the viewpoint of biopharmaceutical modeling.

11.1 SALTS AND COCRYSTALS: SUPERSATURATING API

Salt formation is most widely used as a measure to overcome the dissolution rate and/or solubility-permeability-limited absorptions for dissociable drugs. After dissolution of the salt, a supersaturated drug concentration can be induced in the intestine (Fig. 11.1). This transient supersaturated drug concentration can be

Biopharmaceutics Modeling and Simulations: Theory, Practice, Methods, and Applications, First Edition. Kiyohiko Sugano.

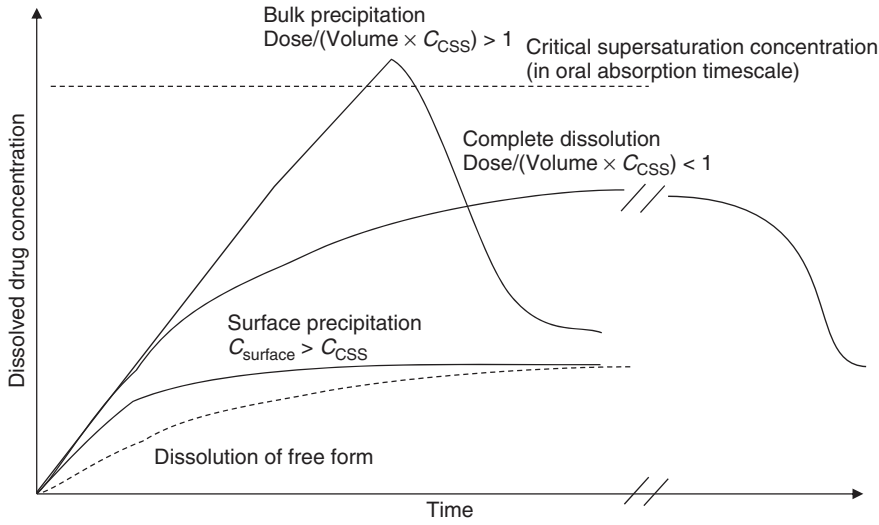

Figure 11.1 Dissolved drug concentration from a salt.

maintained during the intestinal transit time[1] and can enhance the oral absorption of a drug. Figure 11.2 shows the schematic presentation of the dose–AUC profile. In most cases, a salt form significantly outperforms a free form.

For biopharmaceutical modeling of a salt, an appropriate nucleation model is required to predict the precipitation *in vivo*. The use of classical nucleation theory would be just a starting point to incorporate the nucleation process into

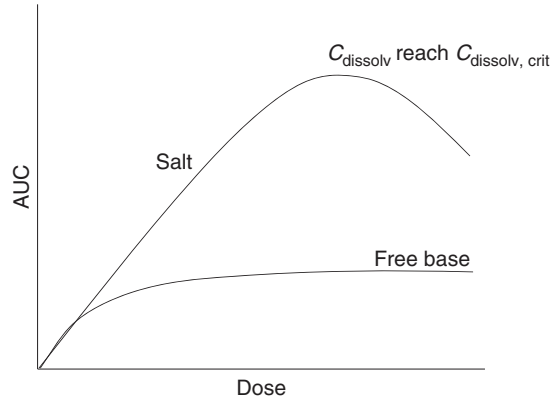

Figure 11.2 Dose–AUC pattern theoretically predicted for a salt.

[1]The equilibrium solubility of a drug at a pH in the pH-controlled region becomes the same value, regardless of the starting material being a salt or a free form (Section 2.3).

biopharmaceutical modeling (Section 3.3). In addition, none of the *in vitro* dissolution models have been successful in predicting the supersaturation *in vivo* [1].[2] The nucleation of a free form can occur not only in the bulk fluid but also at the solid surface of the drug [2–5].

In this section, we first discuss the three possible scenarios for the oral absorption of a salt. Some case examples are then discussed. A case by case strategy of biopharmaceutical modeling is then discussed. The discussion about a salt can be also applicable for cocrystals, anhydrates, and amorphous APIs (supersaturating APIs) (see also spring and parachute approach; Fig. 11.14).

11.1.1 Scenarios of Oral Absorption of Salt

There are several possible scenarios for the oral absorption of a salt (Fig. 11.1) [6].

(A) The dissolved drug concentration (C_{dissolv}) does not reach the critical supersaturation concentration ($C_{\text{dissolv, crit}}$) because the dose is not high enough and/or a high permeation clearance reduces C_{dissolv}. The nucleation induction time is longer than the intestinal transit time. The dose number based on $C_{\text{dissolv, crit}}$ ($\text{Do}_{\text{supersaturation}} = \text{Dose}/(V_{\text{GI}} \times C_{\text{dissolv, crit}})$) is less than 1. Precipitation of the free form does not occur both in the bulk fluid and solid surface.

(B) The nucleation induction time is shorter than the intestinal transit time, but the supersaturated concentration is maintained for several minutes to hours.

(C) As the salt form of a drug dissolves, the concentration of the drug reaches $C_{\text{dissolv, crit}}$ in the GI tract ($\text{Do}_{\text{supersaturation}} > 1$), and a free form immediately precipitates out (mostly as fine particles). The precipitated free form redissolves rapidly (faster than absorption flux), and therefore, C_{dissolv} is maintained at the saturated solubility of the precipitant (free form) during the absorption process. The solid form of the precipitant can be a stable form (crystalline) or semistable form (amorphous).

(D) A free form precipitates out at the surface of dissolving salt as an insoluble layer.

  (D-1) The precipitated free form forms a loose and porous layer on the surface of the salt. The dissolution of the drug continues, however, at a somewhat slower rate than the original salt because of the extra barrier for dissolution.

  (D-2) The precipitated free form completely covers the surface of a salt. Further dissolution is controlled by the solubility of the free form on the solid surface. Although the supersaturable form exists below the surface layer, it is not available for dissolution.

[2]Using a nonsink dissolution test, a rank-order comparison of various salts might be possible.

11.1.2 Examples

11.1.2.1 Example 1: Salt of Basic Drugs. AZ0865 mesylate (45–159 mg/dose) [1] and indinavir sulfate (250–500 mg/m^2) [7] might be the case for scenario (A). In this dose range, the oral absorption of these drugs is dose-linear (Figs. 7.23 and 11.3).

FTI-2600 might be the case for scenario (C). In the *in vitro* dissolution test, after the HCl salt was dissolved, the free base immediately precipitated out in an amorphous form. However, it was not further converted to a crystalline form (Fig. 11.4). In this case, C_{dissolv} in the small intestine is determined by the solubility of the amorphous form.[3]

Ziprasidone HCl and mesylate are also likely to be the cases for scenario (C). The solubility values of these salts in the unbuffered water are 0.08 and 0.73 mg/ml, respectively [9], suggesting that if there is no precipitation, Fa% should be 100% at 40-mg dose in humans. The equilibrium solubility of ziprasidone in a pH 7.4 buffer is 0.0008 μg/ml. The relative bioavailability in humans in the fasted state is ca. 30–50% compared to that in the fed state and other solubility-enhanced formulations (Table 11.1) [10]. At 20–80 mg, the oral absorption is dose-subproportional in the fasted state, but it is dose-proportional in the fed state [11]. These observations suggest that precipitation occurred *in vivo* in the fasted state. As the particle size of the HCl salt had only a little effect on the oral absorption (20 vs 105 μm), it is unlikely that precipitation of the free base occurred at the solid surface (but this is not conclusive) [12]. Interestingly,

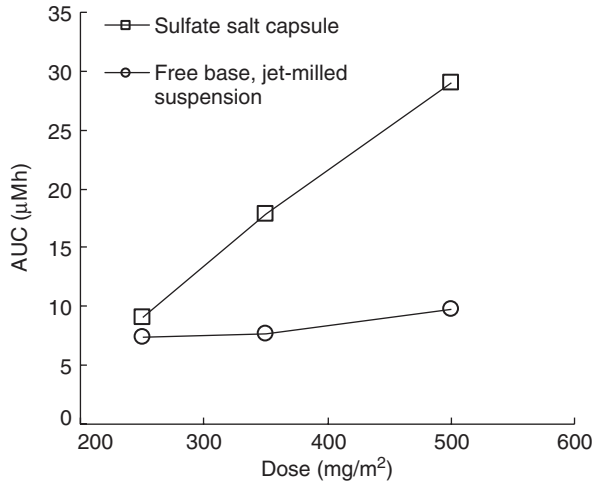

Figure 11.3 Dose dependency of AUC after administration of indinavir sulfate in humans [7].

[3]This concentration could be much higher compared to the solubility of a crystalline form. Therefore, the concentration of the drug is supersaturated against a crystalline.

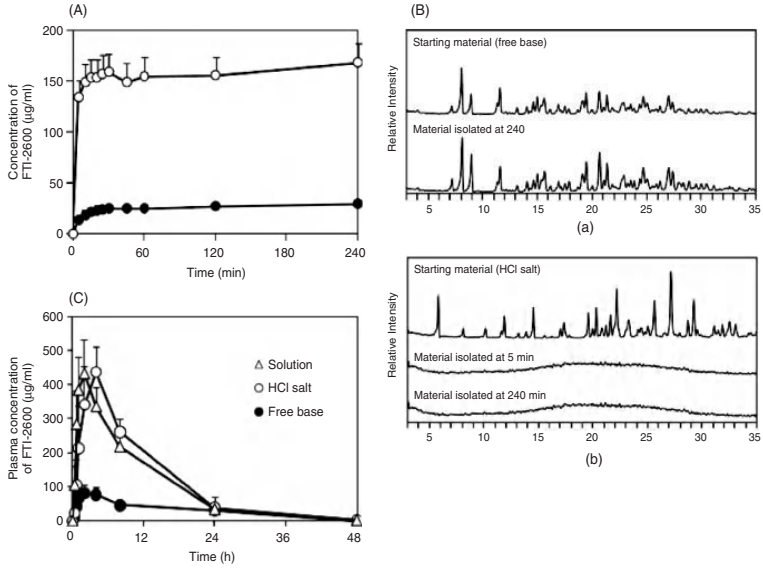

Figure 11.4 FTI-2600. (a) Dissolution profile of FTI-2600 crystalline free base and HCl salt in FaSSIF, (b) PXRD pattern of the initial and precipitated solids. Initial material: (a) crystalline free base and (b) HCl salt. (C) *In vivo* PK profile. Mean ± SD plasma concentrations of FTI-2600 following oral administration in achlorhydric beagle dogs ($n = 5$) under fasted conditions at a dose of 3 mg/kg. Δ, FTI-2600 crystalline free base dissolved in 10% HCO60 solution; ◯, a mixture of FTI-2600 HCl salt and lactose encapsulated in hard gelatin capsules; ●, FTI-2600 crystalline free base suspended in 5% gum arabic. *Source:* Adapted from Reference 8 with permission.

TABLE 11.1 Bioavailabilities of Ziprasidone Salts and Formulations

API	Dose, mg	Formulation	Fasted/Fed	AUC, ng h/ml	BA%	Fa% (Fh Model)	Fa%[a]
HCl	40	Capsule	Fasted	481	23	55	38
HCl	40	HPMC-coated tablet	Fasted	822	39	93	66
Free	40	Nanosuspension	Fasted	962	45	109	77
HCl	20	Capsule	Fed	627	59	142	100

[a] On the basis of the AUC of 20-mg capsule in the fed state.

HPMC (hydroxypropylmethylcellulose) coating significantly increased the oral absorption of the HCl salt probably due to precipitation inhibiting effect of the HPMC polymer [9]. Nanoparticles of the free base also significantly increase the oral absorption of ziprasidone [9].

REV 5901 might be the case for D-2) [2]. The pH–solubility profiles of both the base and the salt at 37°C were identical and were in agreement with a pK_a value of 3.67. The solubility of the drug (ca. 0.002 mg/ml at pH 6) increased gradually with a decrease in pH and reached 0.95 mg/ml at pH 1. At pH < 1, the solubility decreased as a result of the common-ion effect. At pH values greater than pH_{max}, due to the rapid conversion of the salt to the free base at the surface of the salt, the dissolution rates of both the base and the salt were found to be identical.

11.1.2.2 Example 2: Salt of Acid Drugs. It is often speculated that the salt of an acid should have a similar bioavailability with the free acid, as the salt will be immediately converted to a free acid when it comes into contact with the acidic pH in the stomach. However, salt formation often increases the bioavailability of acid drugs with low solubility.

The oral absorption of phenytoin sodium might be the case for scenario (C). Phenytoin is an acidic compound with a pK_a value of 8.4, and its solubility is 35–40 μg/ml at 37°C in the pH range of 1–7.4. Therefore, only about 5 mg of the drug dissolves in the GI fluid (~130 ml) and the excess drug precipitates out in a finely divided state [13]. As shown in Figure 11.5, the oral absorption of phenytoin sodium is significantly higher than that of free acid (of 50–100 μm particle size) at 400-mg dose (5.7 mg/kg) in humans. As no supersaturation was observed in an *in vitro* dissolution test at pH 1.2 and 5 (50 mg in 500 ml), phenytoin sodium would be converted to the free acid immediately in the stomach and/or in the small intestine [14]. Interestingly, the oral absorption from the fine particles of phenytoin free acid (4 μm) and the sodium salt was found to be similar in humans at 280- (4 mg/kg) and 210-mg (3 mg/kg) doses, respectively [14].

In dogs, the oral absorption from phenytoin sodium was ca. twofold higher than that of fine particles (4 μm) at 50 mg/kg [14].

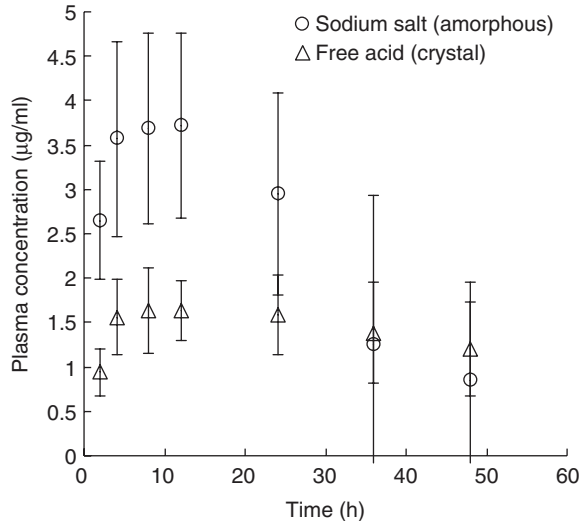

Figure 11.5 Plasma concentration–time profile of phenytoin in humans after administration of 400-mg dose. Sodium salt: amorphous form with 1–3 μm particle size. Free acid: crystalline with 50–100 μm particle size.

11.1.2.3 Example 3: Other Supersaturable API Forms. As an anhydrate has higher solubility than a hydrate, it can induce supersaturation. Figure 11.6 shows the dissolution and the C_p–time profiles of carbamazepine in dogs. The conversion rate from anhydrate to hydrate in the water is slow and is inhibited by the bile-micelles [4]. Four anhydrate forms have been identified [15], and one of them is used in a marketed drug product [16].

Recently, cocrystals attracted a lot of attention in pharmaceutical industries. Implementation of high throughput solid form screening increased the success rate of finding cocrystals [18]. Cocrystals can behave like salts, so that after fast dissolution in the GI tract, a supersaturated concentration can be maintained. However, a limited number of oral absorption data is available in the literature [19–21]. Figure 11.7 shows the case examples for which an increase in oral absorption is observed by forming a cocrystal [16].

An amorphous form is often discussed as the API form to increase Fa%. However, a naked amorphous API is often not stable and is not suitable for drug development. Therefore, the amorphous state is often stabilized as solid dispersion formulations.

11.1.3 Suitable Drug for Salts

11.1.3.1 pK_a Range. For the development of a salt, the balance of bioavailability and storage stability should be considered. Long-term physical and chemical stability over a 2-year period at room temperature is usually required for marketing. For a base drug, no compound with $pK_a < 4.6$ has been marketed as

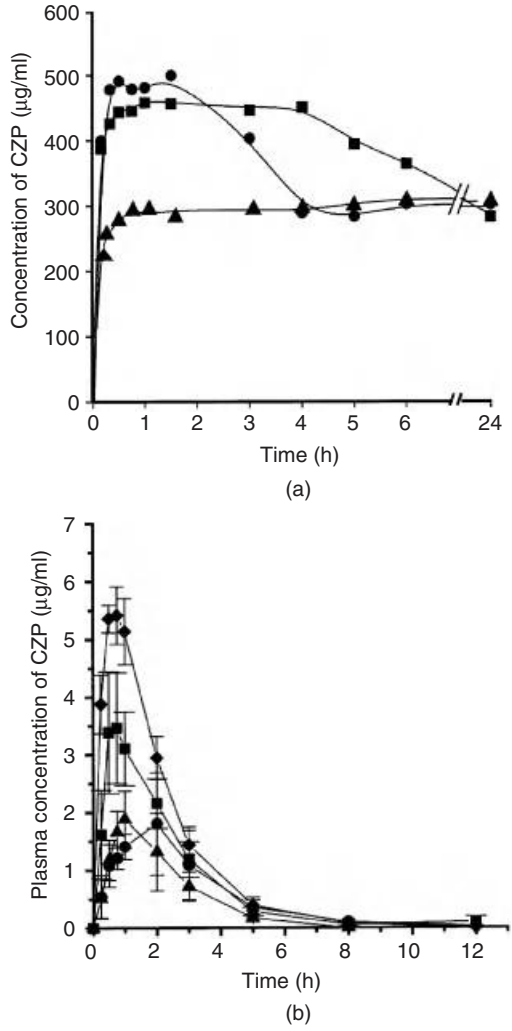

Figure 11.6 (a) Dissolution and (b) C_p-time profiles of carbamazepine polymorphs and dihydrate. (a) pH 1.2 at 37°C under nonsink conditions. (b) Plasma concentration-time curves after oral administration of 400 mg to dogs ($n = 4$; mean ± S.E.). ■, anhydrate form I; ●, anhydrate form III; ▲, dehydrate; and ◆, solution. CZP, carbamazepine. *Source:* Adapted from Reference 17 with permission.

a salt in the past (Tables 11.2 and 11.3) [22]. This does not necessarily mean that a compound with a pK_a < 4.6 cannot be marketed as a salt. But the development of a compound with low pK_a values might be more challenging, as it has an inherent risk of disproportionation. Figure 11.8 shows the pK_a values of drugs and its counterions for the marketed drugs. It is commonly believed that when the difference between the pK_a of an acid and a base is greater than 2, a

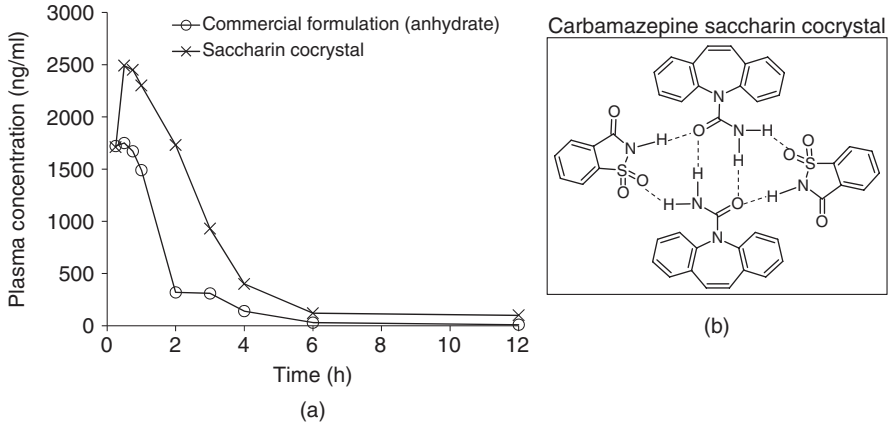

Figure 11.7 C_p–time profiles of carbamazepine (200 mg) in fasted beagle dogs ($n = 4$). (a) Commercial formulation (anhydrate) versus saccharin cocrystal. (b) Structure of carbamazepine–saccharin cocrystal. *Source:* Replotted from Reference 16.

TABLE 11.2 Classification of Acids and Bases According to their Strength[a]

	pK_a	
Attribute	Acids	Bases
Very strong	<0	14
Strong	0–4.5	9.5–14
Weak	4.5–9.5	4.5–9.5
Very weak	9.5–14	0–4.5
Extremely weak	14	<0

[a] Reference 22.

stable salt can be formed ("rule of two") [23]. If the pH_{max} of a salt is lower than the microenvironmental pH of the excipients, the risk of disproportionation (conversion to a free base) becomes higher. Even a small portion of a free base (<0.1%) can induce catastrophic precipitation (Fig. 11.9) [3]. However, quantitative detection of a trace amount of a free base is practically impossible. A nonsink dissolution test may be used to investigate the stability of a salt [24].

11.1.3.2 Supersaturability of Drugs. By the kinetic pH titration method (Section 7.8.1), Box et al. [25] identified some chemical structural characteristics of supersaturable and nonsupersaturable drugs. Typical chemical features are listed in Table 11.4. In the case of nonsupersaturable drugs, an amorphous solid (or oil) precipitated out and this amorphous form did not get converted to a crystalline form during the experimental time.[4] Recently, it was demonstrated that

[4] Salt formation is often used to obtain a crystalline material when the free form does not crystallize. In addition, in the case of a base, salt formation can avoid absorption of CO_2 from the air.

TABLE 11.3 Excipient Microenvironmental pH[a]

Excipient	pH
Dibasic calcium phosphate anhydrous USP (A-Tab granules)	2.21
Dibasic calcium phosphate anhydrous (Sigma Chemicals)	3.59
PVP	3.7
Microcrystalline cellulose NF (Avicel PH102)	4.07
Microcrystalline cellulose JP (Avicel PH101)	4.03
Microcrystalline cellulose NF (Avicel PH105)	4.14
Lactose monohydrate NF (Fast Flo 316, spray-dried)	4.24
Mannitol	4.7
Microcrystalline cellulose	4.7
Sodium starch glycolate NF (Explotab)	4.77
Crospovidone	4.9
Colloidal SiO_2	5.2
Sodium croscarmellose	5–7
Lactose	6.1
Maize starch	6.3
Calcium carbonate USP (Vicron 75-17-FG)	6.58
Magnesium stearate	7.1
Carbonate carbonate USP (Calcipure GCC300)	7.20
Magnesium stearate NF	7.45
Hydrogenated castor oil	7.5
Calcium carbonate USP (Precarb 150)	7.69
Calcium carbonate USP (Vicality Medium PCC)	8.07

[a] Reference 22.

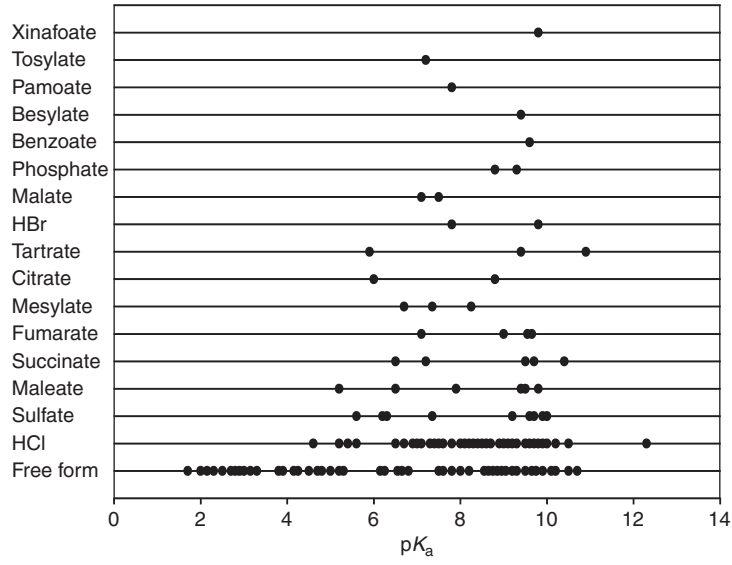

Figure 11.8 Graph depicting the most basic pK_a of an active ingredient versus the counter ion chosen as in its product. *Source:* Adapted from Reference 22 with permission.

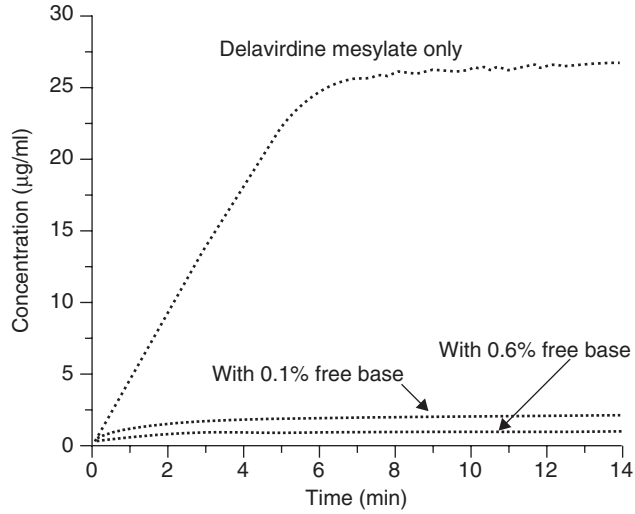

Figure 11.9 Rotating disk dissolution data for delavirdine mesylate at pH 2 spiked with 0%, 0.1%, and 0.6% w/w of delavirdine free base. *Source:* Adapted from Reference 3 with permission.

TABLE 11.4 Typical Features of Chasers and Nonchasers[a]

Supersaturable Drugs	Nonsupersaturable Drugs
• Can be acids, bases, and ampholytes • Sum of H-bond donor + acceptor is 3 or above • Solid form of precipitant tends to be crystalline • High melting point of free form • Solubility usually increases with temperature	• Only observed for bases • Little capacity for H-bonding; most have no H-bond • Low melting point of free form; mainly liquid at 25° C • Solubility unchanged or decreases with temperature

[a] Reference 25.

the nucleation induction time is related to the effectiveness of a supersaturable formulation to increase the oral absorption of a drug [26].

11.1.4 Biopharmaceutical Modeling of Supersaturable API Forms

Given the lack of any appropriate *in vitro* dissolution test and computational model, the current best practice to predict the clinical performance of a salt form is to carefully perform *in vivo* experiments and interpret the data. Dogs would be practically the most appropriate species to investigate the oral absorption of a salt (Section 7.10).

A nonsink *in vitro* dissolution test can be first used to rank-order the performances of salt APIs and other forms (Section 7.8.4). The dose/fluid volume ratio should reflect the clinical situation, as it would affect the extent of supersaturation. The buffer species and capacity would also be critically important to represent the *in vivo* situation. An *in vitro* method tends to underestimate the extent and duration of supersaturation [1]. Gentle stirring without using a paddle is preferable. A stirring bar should not be used, as it artificially induces nucleation by scratching the vessel wall.

On the basis of the results from a nonsink dissolution test, we may be able to follow these strategies for biopharmaceutical modeling.

- If no precipitation is observed in the nonsink dissolution test, biopharmaceutical modeling can be performed by assuming that both S_{dissolv} and S_{surface} are equal to the solubility of the salt ($=K_{\text{sp}}{}^{0.5}$).
- If the dissolution profile shows a high plateau concentration, such as in FTI-2600 (Fig. 11.4) and carbamazepine anhydrate form I (Fig. 11.6), biopharmaceutical modeling can be performed by assuming S_{dissolv} is equal to the plateau concentration and S_{surface} is the theoretical solubility of the administered solid (e.g., $K_{\text{sp}}{}^{0.5}$ for a salt).
- If the dissolution profile of a salt is identical to that of the free form, biopharmaceutical modeling can be performed in the same manner as the free form.
- When the supersaturation duration is within 3.5 h (such as in carbamazepine anhydrate form III; Fig. 11.6), the preexponential and surface energy parameters of the nucleation equation (Section 3.3) can be obtained by curve fitting the *in vitro* data. Then, these parameters are used to estimate the *in vivo* oral absorption.

It should be remembered that *in vitro* tests tend to underestimate supersaturation. Therefore, the above modeling strategy will give a pessimistic estimation. One of the typical mistakes in biopharmaceutical modeling for a salt is that the equilibrium solubility of a salt in a buffer at a pH is used as the solubility input. This would result in a dramatic underestimation of the oral absorption of a salt.

Manufacturability is critically important as well. For robust manufacturing processes and long-term storage stability, it is preferable to select the most stable form among the polymorphs. Salt formation can improve the manufacturability by increasing the stability of the API form [27].

11.2 NANOMILLED API PARTICLES

Nanomilling technology has been proven to be effective in increasing the oral absorption of the solubility-UWL-limited cases, although it is often speculated that nanomilling is only effective in dissolution-rate-limited cases (Fig. 11.10). As discussed in Section 10.2.2, the oral absorption of a drug with low solubility

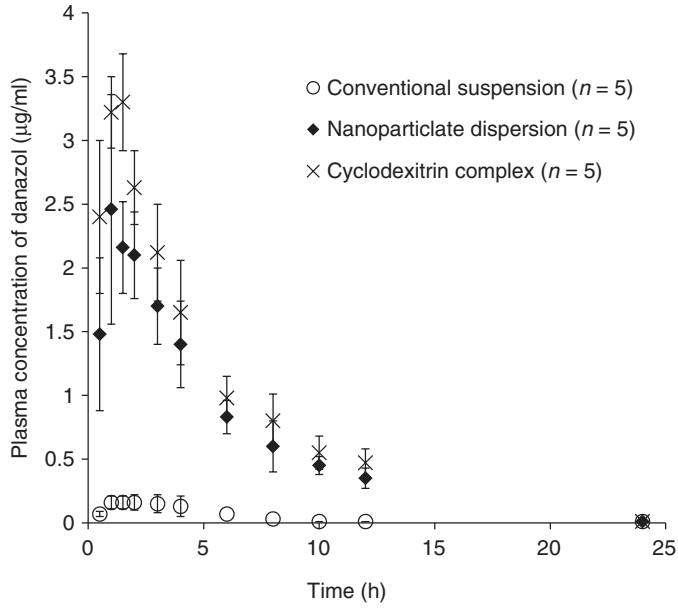

Figure 11.10 Effect of formulations on the oral absorption of danazol in fasted dogs (20 mg/kg). The particle sizes of conventional and nanosuspension were 10 and 0.16 μm, respectively. *Source:* Adapted from Reference 31 with permission.

becomes solubility-permeability limited when the dose is larger than 20 mg and particle size is smaller than 10 μm. Considering the dose of many drugs with low solubility (Table 8.3), the oral absorption of these drugs should be solubility-permeability limited. In addition, an increase in solubility by nanosizing (cf. the Ostwald–Freundlich equation) was also speculated as the reason for enhancing oral absorption. However, this mechanism is unlikely both theoretically and experimentally. The Ostwald–Freundlich equation predicts that this effect becomes significant only when the particle size is less than 100 nm even assuming highest surface tension for a drug (such as that of alkanes) (Section 2.3.9). This point was recently experimentally confirmed for drugs with low solubility (Section 7.6.3.4).

As an alternative explanation, the particle drifting effect (PDE) was introduced (Section 4.7.2). API particles can be drifted into the UWL, and the drug molecules diffuse into the epithelial membrane from the surface of the API particles in the UWL. Even though the PDE was first introduced to explain the oral absorption of SL-U drugs from conventional formulations, this effect would be larger for nanoparticles.

Figures 10.4 and 10.5 show simulated Fa% of danazol and cilostazol in dogs. Introduction of the PDE significantly decreased the discrepancy between simulated and observed Fa%. The Fa% of atovaquone, fenofibrate, and aprepitant nanoparticle formulations was also appropriately simulated (Table 8.3).

The beads mill method has been widely used to prepare a nanomilled formulation in drug discovery and development [28–30]. A drug API is suspended in an aqueous media and strongly stirred with beads. Glass beads and zirconium beads are often used. A polymer is usually added to avoid aggregation of nanomilled particles. The size of the API can be monitored during the milling process, for example, using DLS. After milling, the beads are removed by filtration. The particle size can be reduced to a few hundred nanometer range depending on the property of the API.

11.3 SELF-EMULSIFYING DRUG DELIVERY SYSTEMS (MICELLE/EMULSION SOLUBILIZATION)

The micelle and emulsion solubilization system has been used for many drugs. These formulations are often referred to as *self-emulsifying drug delivery systems* (*SEDDS*). SEDDS can be categorized into four types, depending on the composition of the formulation (Table 11.5) [32]. The formulation type should be selected not only by the biopharmaceutical performance but also by the manufacturability. Solubility in liquid excipients often limits the maximum dose strength, especially for a type I SEDDS formulation.

Once in contact with the GI fluid, the SEDDS forms dispersed micelles. For type I and II formulations, bile-micelle solubilization and the digestion of lipid components by lipase largely affect the performance of these formulations (Fig. 11.11) [33]. The drug concentration in the mixed micelle phase after digestion of the formulation was found to correlate with the exposure of a drug [32, 34]. After entering the intestinal enterocytes, a lipophilic compound of log $P_{oct} > 5$ can be carried by the lymphatic system (Fig. 11.12) [35, 36]. The lymphatic flow is significantly slower than the blood flow. Therefore, the appearance of the drug in the systemic circulation is usually slow. It is well known that the lipid components affect the lymphatic absorption. For example in rats, the lymphatic absorption of halofantrine is 2%, 6%, and 16% from the short-, medium-, and long-chain fatty acid triglyceride formulations, respectively (Table 11.6) [37]. The liver first-pass effect can be avoided via lymphatic transport.

Owing to its complex absorption mechanism, no mechanistic computational modeling has been reported (as of 2011). Construction of an *in vitro* model is also challenging. Therefore, preclinical animal models would be required to assess the performance of SEDDS formulations. The droplet size of emulsions (especially after lipid digestion) seems to have a significant effect on their performance. The drug molecules dissolved in micelles with less than 400 nm size were suggested to be effective for permeation, probably because it can readily defuse the UWL.

Micelle-solubilized drugs can diffuse the UWL, and the unbound fraction of a drug can then permeate the epithelial membrane [35]. Therefore, the UWL and unbound fraction should be at least taken into account for biopharmaceutical modeling of SEDDS. The micelle size (hence diffusion coefficient) could change depending on the excipient component, lipid digestion, and interaction

TABLE 11.5 Type I, II, IIIA, and IIIB Lipid Formulations

Type	I	II	IIIA	IIIB	IV
Typical composition, %					
Triglycerides or mixed glycerides	100	40–80	40–80	<20	—
Water-insoluble surfactants (HLB <12)	—	20–60	—	—	0–20
Water-soluble surfactants (HLB >12)	—	—	20–40	20–50	30–80
Hydrophilic cosolvents (e.g., PEG)	—	—	0–40	20–50	0–50
Oral absorption characteristics					
Particle size of aqueous dispersion, nm	Coarse	100–250	100–250	50–100	50–100
Loss of solubilization capacity	Solvent capacity unaffected	Solvent capacity unaffected	Some loss of solvent capacity	Potential loss of solvent capacity	Potential loss of solvent capacity
Requirement of lipase digestibility	Crucial	Not crucial but likely to occur	Not crucial but may be inhibited	Not required and unlikely to occur	Not required and unlikely to occur

Abbreviation: HLB, hydrophilic–lipophilic balance.

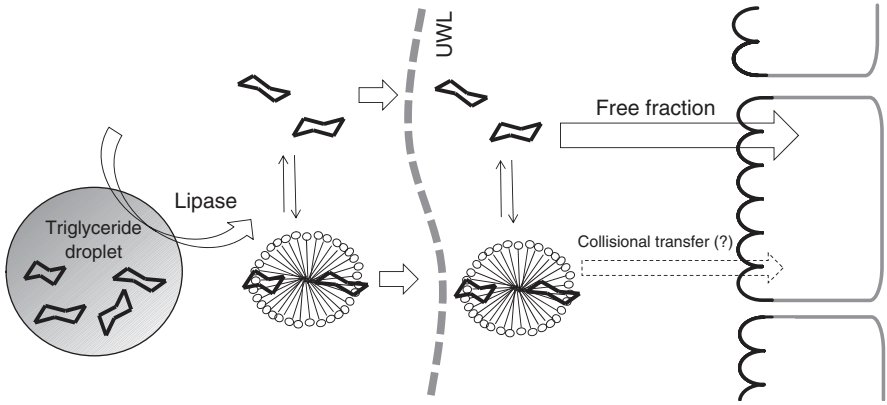

Figure 11.11 Oral absorption process of the lipid-based formulations.

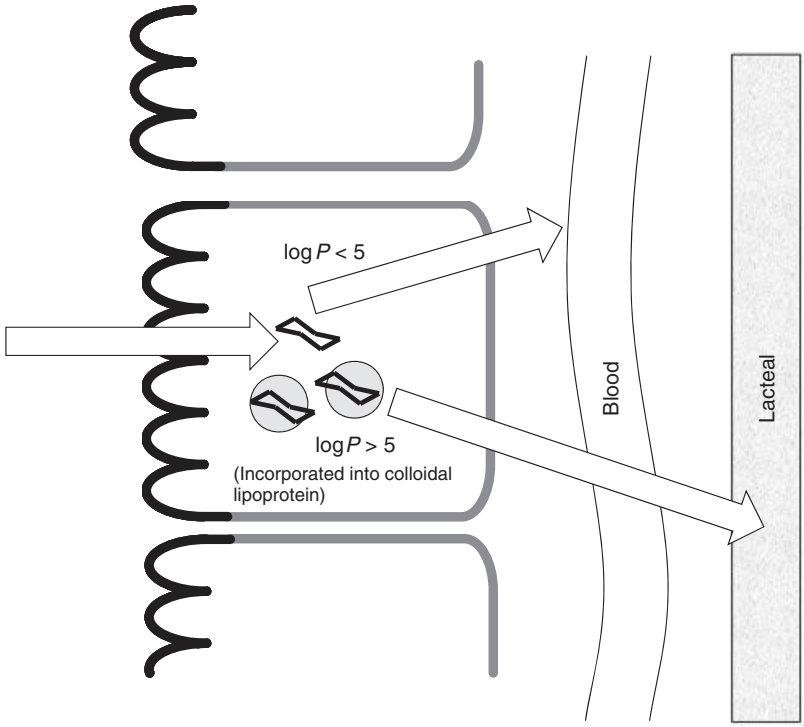

Figure 11.12 Lymphatic absorption [35, 36].

with endogenous bile-micelles. The unbound fraction of a drug in the mixed micelle phase after digestion by lipase should also be considered (Fig. 11.13). If the drug is absorbed via the lymphatic route, the lymphatic flow rate should be taken into account. Even though an API drug is fully solubilized in the

TABLE 11.6 Bioavailability of Halofantrine Free Base (Mean% Dose ± SD, $n = 4$) in Lymph-Cannulated Rats after Oral Administration[a]

Formulation	Lymphatic Transport	Total
LCT (C_{18})	15.8 ± 2.2	22.7 ± 4.0
MCT (C_{8-10})	5.5 ± 1.5	19.2 ± 4.5
SCT (C_4)	2.2 ± 1.8	15.2 ± 3.1
Aqueous suspension	0.34 ± 0.5	6.4 ± 0.8

Cumulative mass of halofantrine recovered over 12 h in mesenteric lymph calculated as a percentage of dose.

The lymph flow (g/12 h) in each experimental group was $13.8 \pm 2.2, 10.0 \pm 2.8, 7.82 \pm 0.7$, and 4.20 ± 2.2 g/12 h, respectively, for groups dosed with LCT, MCT, SCT, or the aqueous suspension formulation.

[a] Reference 37.

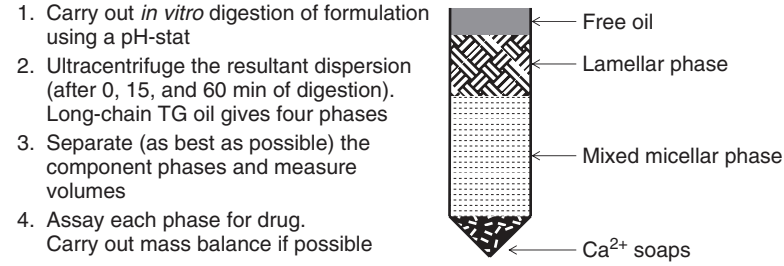

Figure 11.13 Lipase digestion study and components of digestion. TG, triglyceride. *Source:* Adapted from Reference 32 with permission.

formulation, after dispersed in the GI fluid, it can precipitate out in the GI tract. Simulation of this precipitation phenomenon is also a challenging area.

11.4 SOLID DISPERSION

It is well known that solid dispersions and amorphous formulations can significantly improve the oral absorption of drugs with low solubility [38, 39]. As this type of formulations can increase the unbound drug concentration, it would be effective for both SL-E and SL-U cases [40]. Drugs can also exist in the polymer micelles after the erosion of solid dispersion. For biopharmaceutical modeling, considering the proposed mechanism of oral absorption from solid dispersion [40], both unbound molecules and polymer-micelle-bound molecules should be explicitly taken into account. Owing to its complex absorption mechanism, no mechanistic computational modeling has been reported in the literature (as of 2011).

Solid dispersions can be prepared by spray drying, freeze-drying, rapid evaporation, etc. The drug API is dissolved in an organic solvent with polymers, and

then the organic solvent is removed. Freeze-drying and rapid evaporation would be a convenient method to prepare a small-scale sample. A miniscale spray dryer is commercially available and can be used in drug discovery. Hot melt extrusion can also be used to prepare a solid dispersion. As a polymer, HPMC, HPMC-AS, PVP, etc. are often used.

One drawback of the solid dispersion formulation is its storage stability. Crystallization is often observed during storage, resulting in a change in the dissolution profile. It could be kinetically stable to survive more than 2 or 3 years, but a large amount of polymer would be required to stabilize the formulation. Prediction of long-term stability of solid dispersion is a challenging area.

When administering the solid dispersions as a suspension in an aqueous media, the stability of the solid dispersion in the vehicle should be carefully checked. A rapid crystallization is often observed. In addition, dissolution performance should be checked by a dissolution test. A nonsink dissolution test should be used to investigate the supersaturation duration.

11.5 SUPERSATURABLE FORMULATIONS

The concept of supersaturable formulation emerged recently [41–44]. The difference between supersaturated[5] and supersaturable formulations is that the latter one is in itself thermodynamically stable but induces supersaturated drug concentration once dissolved in the intestinal fluid. Figure 11.14 shows the spring and parachute concept for the supersaturable formulations.

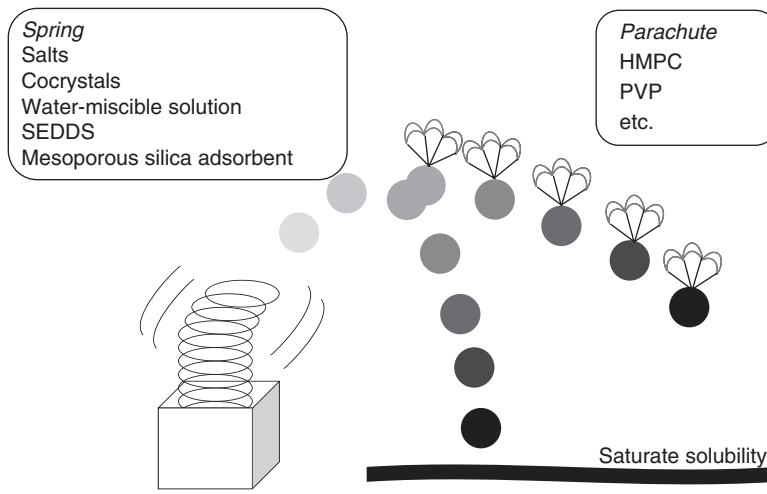

Figure 11.14 Spring and parachute concept.

[5]For example, solid dispersion.

Salts, cocrystals, liquid formulation (including type IV SEDDS), and mesoporous silica adsorbents [45–49] have been used as the "spring" to induce the supersaturated drug concentration [44]. Various polymers have been used to prolong the duration of supersaturation ("parachute"). As this type of formulation can increase the unbound drug concentration, it would be effective for both SL-E and SL-U cases. For biopharmaceutical modeling, the nucleation theory should be taken into account. However, little is known about the mechanism of the inhibition of supersaturation by a polymer. Inhibition of nucleation process was previously suggested as an inhibition mechanism. However, recently, inhibition of crystal growth was suggested as an inhibition mechanism as well [50]. Biopharmaceutical modeling for supersaturable formulations is the subject of future investigation.

11.6 PRODRUGS TO INCREASE SOLUBILITY

To increase the aqueous solubility of drugs with low solubility, a hydrophilic group can be attached to a drug molecule. A phosphate prodrug has been used to increase the solubility of amprenavir (fosamprenavir) (Fig. 11.15). The phosphate moiety is cleaved to the parent drug at the surface of the epithelial membrane, which then permeates the epithelial membrane.

The oral absorption of phenytoin was found to be significantly increased by water-soluble prodrugs (Table 11.7) [51, 52]. Solubility of these phenytoin prodrugs are ca. 150 mg/ml (cf. the solubility of free acid is 0.04 mg/ml).

Biopharmaceutical modeling of the oral absorption of this type of prodrug has not been reported. The rat mucous layer scrap and Caco-2 cells were found to cleave the phosphate prodrug, whereas MDCK cells do not [53].

11.7 PRODRUGS TO INCREASE PERMEABILITY

Practically, a formulation approach to improve membrane permeability has not been successful in the past[6] because an effective enhancer often shows toxicity

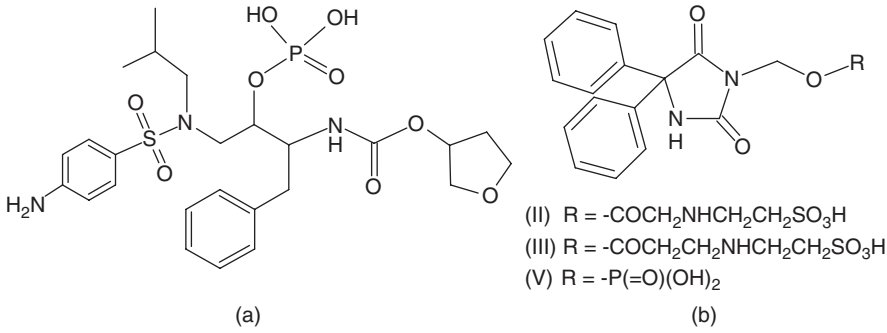

Figure 11.15 Prodrugs to improve solubility: (a) fosamprenavir and (b) phenytoin prodrugs [51, 52].

[6]Capric acid formulation for rectal administration is an exception.

TABLE 11.7 Bioavailability of Phenytoin Prodrugs

	BA%
Prodrug II	65 ± 23
Prodrug III	76 ± 45
Prodrug IV	51 ± 6
Sodium salt	14 ± 3
Free acid	10[a]

[a]Predicted value for 190 μm.

to the intestine. Therefore, prodrug approaches are usually pursued to improve the membrane permeability of a drug.

11.7.1 Increasing Passive Permeation

Most of the prodrugs in the market were designed to increase the passive transcellular permeation of a parent drug by masking hydrophilic functional groups, such as carboxyl, hydroxyl, and guanidine groups [54, 55]. In many cases, prodrugs are converted to the parent drugs by esterase [54]. Animal models may not be suitable to evaluate the performance of a prodrug due to the species difference in carboxyl esterase [54]. In addition, Caco-2 cells express different types of carboxyl esterase from the *in vivo* human intestine [54, 56, 57].

Although not yet investigated, biopharmaceutical modeling will be soon applicable for prodrugs. Estimation of the conversion rate in the intestinal lumen and enterocyte is of particular importance. Mizuma [58] summarized the relationship between the conversion clearance and absorption clearance.

11.7.2 Hitchhiking the Carrier

Valacyclovir is a prodrug of acyclovir (Fig. 11.16) [59]. Valacyclovir is designed to hitchhike PEP-T1 expressed in the small intestine. This approach has been extensively investigated [60–64]. In addition to PEP-T1, bile acid transporter [62] and glucose transporter [65–67] were also investigated as a candidate for this approach.

11.8 CONTROLLED RELEASE

Biopharmaceutical modeling for controlled-release (CR) formulations is one of the most highly demanded tasks for biopharmaceutical modeling. CR can be categorized as prolonged release, timed release, and stimuli-triggered release. A prolonged-release formulation is designed to gradually release a drug. A timed-release formulation is designed to release a drug at a predefined time elapsing after administration. The stimuli-triggered formulations, such as an enteric coating formulation, are designed to release a drug by a specific stimulus at the desired GI

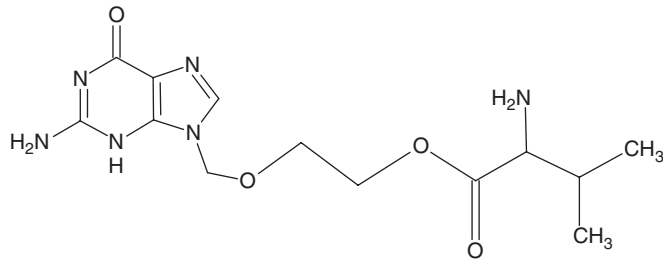

Figure 11.16 Valacyclovir.

position, for example, pH. In the following sections, each category is discussed in detail, as well as the key aspects of biopharmaceutical modeling.

The objectives of biopharmaceutical modeling for a CR development can be divided into (A) mechanistic simulation of release profile from the formulation and (B) convolution of the release pattern with the PK profile. For (A), various factors had to be taken into account, for example, the mechanism of water penetration into the formulation, erosion of the excipient, dissolution of a drug, and the effect of shear force. This type of investigation is important for designing the formulation and manufacture process. On the other hand, (B) is often used to figure out the release pattern required to achieve a desirable PK profile. Even though (A) and (B) can be merged in the future, currently these two are separately investigated. In the following sections, we first discuss (B) and then briefly discuss (A).

11.8.1 Fundamentals of CR Modeling

For a CR formulation to work, the following two points are fundamental:

- CR formulation is designed to show a robust release profile against the variations in the physiological environment, such as pH, bile concentration, and agitation strength.
- The rate-limiting process of drug absorption should be the drug release process from the formulation, rather than intestinal membrane permeability.

These trivial points mean that the use of complicated physiological biopharmaceutical modeling is not required in most cases. Even though the CR function is provided in commercial modeling software, these programs only calculate the convolution of user-defined release profile and PK profile. Currently, little or no mechanistic biopharmaceutical modeling has been reported, in which the effect of physiological environment on the release profile of CR formulation has been taken into account. Therefore, a convolution of drug release and drug disposition functions might be sufficient for biopharmaceutical modeling (the use of a complicated physiological GI model may not be required or should even be avoided considering the transparency of the model).

11.8.2 Simple Convolution Method

A simple configuration, such as zero-order release/dissolution function plus one compartment PK model, would be sufficient for many cases. The release/dissolution function can be selected based on the *in vitro* release/dissolution profile of the formulation. Therefore, the success of biopharmaceutical modeling is critically dependent on the dissolution test conditions. It is well known that the buffer species used in a dissolution test can have significant impact on the release/dissolution profile of a CR formulation. A phosphate buffer, which is most widely used as a dissolution media (including FaSSIF and FeSSIF), may not be suitable, whereas a bicarbonate buffer would be more suitable [68, 69].

11.8.3 Advanced Controlled-Release Modeling

It is very difficult to incorporate the effect of biological factors into the modeling of CR formulation. To do this task, a mechanistic model that can handle the effect of physiological factors on the release profile is required. Currently, mechanistic simulation of drug release from a matrix-type CR formulation is under extensive investigation [70–72]. Jia and Williams used the computational fluid dynamic (CFD) simulation to investigate the dissolution behavior of a tablet. X-ray micro-tomography (XMT) was used to provide the structural input [73] for CFD.

11.8.4 Controlled-Release Function

In biopharmaceutical modeling, the release profile can be represented by a CR function, which is linked to the virtual particle bins (Section 5.4.3). For prolonged- and timed-release formulations, the binary CR function can be programmed to activate the dissolution of the particles as a function of time after oral administration. For triggered-release formulations, the binary CR function can be programmed to activate the dissolution of the particle by a specific physiological condition or elapsed time, such as pH (Section 5.4.3).

11.8.5 Sustained Release

11.8.5.1 Objectives to Develop a Sustained-Release Formulation. The key objectives for prolonged release could be to

- reduce the dosing frequency to increase compliance;
- decrease the systemic side effects by lowering the C_{max}/C_{min} ratio;
- avoid degradation by the acidic pH of the stomach;
- deliver the drug to fit to the circadian rhythm of a disease.

If CR is needed to reduce C_{max}-related side effects, the dosage form might have a 4–6 h delivery duration. If the objective is to avoid degradation of acid-labile drugs, enteric coating formulations can also be used. The timed- or prolonged-release formulation can be used to adjust the C_p–time profile with the circadian rhythm of a disease.

11.8.5.2 Suitable Drug Character for Sustained Release. Feasibilities of a drug for a CR formulation are summarized in Table 11.8 (except enteric coating formulation) [74]. Among these properties, mathematical biopharmaceutical models can support the assessment of P_{eff}, absorption mechanism, first-pass metabolism, etc. The drug should have reasonable solubility and permeability along the GI tract. The assessment of regional differences is discussed in detail in Section 13.6.

11.8.5.3 Gastroretentive Formulation. The gastroretentive formulation gained a lot of interest, as it can continuously supply drug to the upper small intestine. Therefore, this technology can be applied to a drug that shows site-specific and/or saturable membrane permeation in the upper small intestine, especially the ones with little colonic absorption, such as gabapentin (Fig. 11.17). Ofloxacin, metformine, ciprofloxacin, gabapentin, morphine, prazosin, cefaclor, tramadol, baclofen, carvedilol, levodopa, diazepam, and misoprostol have been marketed as gastroretentive formulation [75].

Swelling [77] and floating [75] systems are most often used. The swelling system formulation increases its size larger than the pylorus diameter when it is exposed to the gastric fluid. As erosion of the swelled formulation occurs, the size of the formulation reduces and the formulation eventually exits into the small intestine. The initial formulation size is typically ca. 10 mm, and the size expands a few fold in the stomach.

The floating system has sufficient buoyancy to float over the gastric contents and remain in the stomach for a prolonged period. While the system floats over the gastric contents, the drug is slowly released [75]. Floating systems can be further classified as effervescent and noneffervescent systems.

Biopharmaceutical modeling would be beneficial to support the design of release profile. The gastric emptying time of a formulation can be modified to represent the *in vivo* situation.

11.8.6 Triggered Release

11.8.6.1 Time-Triggered Release. Time-triggered release (pulsate release) is of particular interest for chronotherapy [78, 79]. Single unit and multiple unit systems have been investigated. Biopharmaceutical modeling for multiple unit systems are straightforward, as the release from a granule can be easily represented by the conditional binary CR function (Section 5.4.3). For single unit system, the migrating motor complex affects the gastric emptying time (Section 6.2.2).

11.8.6.2 pH-Triggered Release. Enteric coating is often used to avoid degradation of a drug in the stomach and/or to protect the stomach from irritation by a drug. The coating polymer is usually an acid polymer that does not dissolve at an acidic pH but dissolves in a neutral pH of around 5–6. Polymethacrylic resins are widely used as pH-sensitive polymers for the purpose

TABLE 11.8 Suitability for Controlled-Release Formulation

Dose, mg	<1	Greater development complexity (potential drug content uniformity issue)
	10–250	Average degree of difficulty
	≫250–300	Could need more than one tablet to accommodate the drug load
Dose Number	<0.004	Several technology options exist for CR development
	0.004<, <0.4	Average degree of difficulty
	0.4<, <4	CR development will be challenging but feasible
	4<, <40	Need solubilization; CR development will be difficult
	>40	CR development is practically impossible
Absorption Mechanism	Transcellular passive diffusion	Average degree of difficulty
	Other mechanisms including efflux	Performance could be difficult to predict
Permeability (P_{eff}), cm/s	$< 0.3 \times 10^{-4}$	CR formulations with prolonged delivery duration may not be feasible; likely will not be bioequivalent to IR
	$0.3<, <3 \times 10^{-4}$	CR development challenging but feasible; might not be bioequivalent to IR
	$>3 \times 10^{-4}$	CR development should be feasible; likely to be bioequivalent to IR
Metabolism and Efflux	High presystemic or first-pass metabolism	Relative BA of CR formulation might be low
	Compound is P-gp or CYP3A4 substrate	CR performance difficult to predict
PK or PD Half-Life	<1–2 h	Half-life too short for CR development
	2–10 h	Acceptable half-life
	>10 h	Compound might not need CR for reducing dosing frequency

IR, immediate release.

of enteric coating and colon targeting, for example, commercially available ones such as Eudragit®. Different types of Eudragit, whether water insoluble or water soluble, are used for colon targeting. Eudragit L dissolves at pH $\geq$ 6, whereas Eudragit S dissolves at pH $\geq$ 7 because of the presence of a higher amount of esterified groups than carboxylic groups.

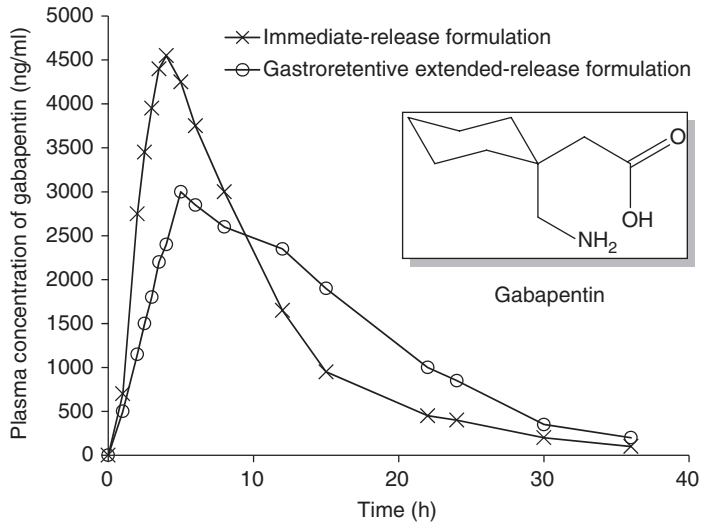

Figure 11.17 Gabapentin plasma concentration (mean ± SE)-time profiles following single-dose oral administration of the drug (600 mg) as immediate-release and gastroretentive extended-release formulations under fed state (1000 kcal, ~50% from fat). *Source:* Replotted from Reference 76.

The pH-triggered formulation for colonic targeting has been investigated. Compared to enteric coating, colon targeting by a pH-sensitive polymer is difficult because of the intra- and interindividual variation in the intestinal and colonic pH.

Biopharmaceutical modeling for pH-sensitive formulations is relatively straightforward. The CR function can be programmed to activate as the virtual particle bins sense the pH environment (Section 5.4.3). The postprandial pH change in the stomach should be taken into account when investigating the food effect on the pH-triggered CR formulation.

11.8.6.3 Position-Triggered Release. The diazo functional group is liable for bacterial degradation in the colon. This property can be used to deliver an active drug to the colon. The prodrug approach has been most successful in the past, for example, sulfasalazine. Bacteria-degradable polymers have also been investigated [80, 81]. Biopharmaceutical modeling can be performed in the same manner with the pH-triggered formulation.

11.9 COMMUNICATION WITH THERAPEUTIC PROJECT TEAM

Biopharmaceutical modeling is often requested from a project team to investigate the feasibility of enabling formulations. This request should be responded starting with consultation. In more than 50% cases, probably more than 80% cases, the

requests from a project team can be solved without actually performing biopharmaceutical modeling. For example, the CR feasibility table (Table 11.8) can be used as the guidance. Discovery project teams tend to place too much hope on enabling formulations and biopharmaceutical modeling, as they are often exposed to exaggerated advertisements about the capability of these technologies. The subject matter experts should objectively communicate the pros and cons of these techniques to the discovery project teams.

The first step is to listen to the customers and work together to derive a problem statement. In many cases, the customer is not aware of the true problem and simply asks us to run biopharmaceutical modeling. We should first discuss various perspectives of the project (e.g., target disease, patient population, available PK and physicochemical data, and deadline). The second step is to identify the cause of inappropriate exposure. Biopharmaceutical modeling will be helpful to quantitatively identify the cause of inappropriate exposure from a standard formulation. If the cause is a metabolic clearance process, enabling formations cannot be helpful (an alternative administration route may work). The third step is to identify the suitable enabling formulations for the drug (Fig. 11.18).

The last step is the assessment of the effect of an enabling formulation on oral absorption of a drug. However, because the absorption enhancement mechanisms of the enabling formulations are complicated, biopharmaceutical modeling might not be applicable. In addition, there might not exist any appropriate *in vitro* method. Therefore, an *in vivo* test should also be considered. In the preclinical stage, *in vivo* dog models would be practically the most appropriate method to test the performance of formulations. These points should be well communicated to the other disciplines that are overexpecting the ability of current commercial biopharmaceutical modeling programs.

For CR simulation, the tabled data of release profile obtained from an *in vitro* dissolution test is often used for simulation. When a commercial program is used in this way, it should be remembered that the effect of physiological factors are

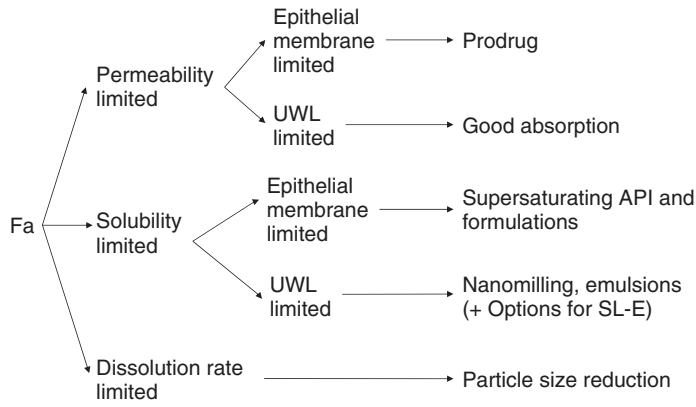

Figure 11.18 Decision tree for enabling formulation.

not taken into account for the release profile from the formulation. A simple combination of release kinetics and disposition kinetics would be sufficient for many cases, as the dissolution (of API) and membrane permeability is usually not the rate-limiting step for a CR drug product.

REFERENCES

1. Carlert, S., Palsson, A., Hanisch, G., von Corswant, C., Nilsson, C., Lindfors, L., Lennernas, H., Abrahamsson, B. (2010). Predicting intestinal precipitation–a case example for a basic BCS class II drug. *Pharm. Res*., 27, 2119–2130.
2. Serajuddin, A. T., Sheen, P. C., Mufson, D., Bernstein, D. F., Augustine, M. A. (1986). Preformulation study of a poorly water-soluble drug, alpha-pentyl-3-(2-quinolinylmethoxy)benzenemethanol: selection of the base for dosage form design. *J. Pharm. Sci*., 75, 492–496.
3. Hawley, M., Morozowich, W. (2010). Modifying the diffusion layer of soluble salts of poorly soluble basic drugs to improve dissolution performance. *Mol. Pharm*., 7, 1441–1449.
4. Lehto, P., Aaltonen, J., Tenho, M., Rantanen, J., Hirvonen, J., Tanninen, V. P., Peltonen, L. (2009). Solvent-mediated solid phase transformations of carbamazepine: effects of simulated intestinal fluid and fasted state simulated intestinal fluid. *J. Pharm. Sci*., 98, 985–996.
5. Boetker, J. P., Savolainen, M., Koradia, V., Tian, F., Rades, T., Mullertz, A., Cornett, C., Rantanen, J., Ostergaard, J. (2011). Insights into the early dissolution events of amlodipine using UV imaging and Raman spectroscopy. *Mol. Pharm*., 8, 1372–1380.
6. Serajuddin, A. T. M. (2007). Salt formation to improve drug solubility. *Adv. Drug Delivery Rev*., 59, 603–616.
7. Mueller, B. U., Sleasman, J., Nelson, R. P. Jr., Smith, S., Deutsch, P. J., Ju, W., Steinberg, S. M., Balis, F. M., Jarosinski, P. F., Brouwers, P., Mistry, G., Winchell, G., Zwerski, S., Sei, S., Wood, L. V., Zeichner, S., Pizzo, P. A. (1998). A phase I/II study of the protease inhibitor indinavir in children with HIV infection. *Pediatrics*, 102, 101–109.
8. Takano, R., Takata, N., Saitoh, R., Furumoto, K., Higo, S., Hayashi, Y., Machida, M., Aso, Y., Yamashita, S. (2010). Quantitative analysis of the effect of supersaturation on in vivo drug absorption. *Mol. Pharm*., 7, 1431–1440.
9. Busch, F. R., Rose, C. A., Shine, R. J. (1999). Mesylate dihydrate salts of 5-(2-(4-(1,2-benzisothiazol-3-yl)-1-piperazinyl)-ethyl)-6-chloro-1,3-dihyd ro-2(1H)-indol-2-one (= ziprasidone), its preparation and its use as dopamine D2 antagonist.
10. Curatolo, W. J., Herbig, S. M., Hombre, A. G., Shah, J. C., Shamblin, S. L., Lukas, T., Caldwell, W. B., Friesen, D. T., Lyon, D. K., Craig, C. D. (2009). Methods, dosage forms and kits for administering ziprasidone without food.
11. Miceli, J. J., Glue, P., Alderman, J., Wilner, K. (2007). The effect of food on the absorption of oral ziprasidone. *Psychopharmacol. Bull*., 40, 58–68.
12. Arenson, D. R., Busch, F. R., Hausberger, A. G., Rasadi, B. (1999). Ziprasidone formulations.

13. Dill, W. A., Glazko, A. J., Kazenko, A., Wolf, L. M. (1956). Studies on 5, 5′-diphenylhydantoin (dilantin) in animals and man. *J. Pharmacol. Exp. Ther*., 118, 270–279.

14. Shinkuma, D., Hashimoto, H., Yamanaka, Y., Murata, Y., Mizuno, N. (1979). Bioavailability of phenytoin. *Yakugaku Zasshi*, 39, 121–128.

15. Grzesiak, A. L., Lang, M., Kim, K., Matzger, A. J. (2003). Comparison of the four anhydrous polymorphs of carbamazepine and the crystal structure of form I. *J. Pharm. Sci*., 92, 2260–2271.

16. Hickey, M. B., Peterson, M. L., Scoppettuolo, L. A., Morrisette, S. L., Vetter, A., Guzman, H., Remenar, J. F., Zhang, Z., Tawa, M. D., Haley, S., Zaworotko, M. J., Almarsson, O. (2007). Performance comparison of a co-crystal of carbamazepine with marketed product. *Eur. J. Pharm. Biopharm*., 67, 112–119.

17. Kobayashi, Y., Ito, S., Itai, S., Yamamoto, K. (2000). Physicochemical properties and bioavailability of carbamazepine polymorphs and dihydrate. *Int. J. Pharm*., 193, 137–146.

18. Takata, N., Shiraki, K., Takano, R., Hayashi, Y., Terada, K. (2008). Cocrystal screening of stanolone and mestanolone using slurry crystallization. *Cryst. Growth Des*., 8, 3032–3037.

19. McNamara, D. P., Childs, S. L., Giordano, J., Iarriccio, A., Cassidy, J., Shet, M. S., Mannion, R., O'Donnell, E., Park, A. (2006). Use of a glutaric acid cocrystal to improve oral bioavailability of a low solubility API. *Pharm. Res*., 23, 1888–1897.

20. Bak, A., Gore, A., Yanez, E., Stanton, M., Tufekcic, S., Syed, R., Akrami, A., Rose, M., Surapaneni, S., Bostick, T., King, A., Neervannan, S., Ostovic, D., Koparkar, A. (2008). The co-crystal approach to improve the exposure of a water-insoluble compound: AMG 517 sorbic acid co-crystal characterization and pharmacokinetics. *J. Pharm. Sci*., 97, 3942–3956.

21. Jung, M. S., Kim, J. S., Kim, M. S., Alhalaweh, A., Cho, W., Hwang, S. J., Velaga, S. P. (2010). Bioavailability of indomethacin-saccharin cocrystals. *J. Pharm. Pharmacol*., 62, 1560–1568.

22. Stephenson, G. A., Aburub, A., Woods, T. A. (2011). Physical stability of salts of weak bases in the solid-state. *J. Pharm. Sci*., 100, 1607–1617.

23. Childs, S. L., Stahly, G. P., Park, A. (2007). The salt-cocrystal continuum: the influence of crystal structure on ionization state. *Mol. Pharm*., 4, 323–338.

24. Gu, C. H., Gandhi, R. B., Tay, L. K., Zhou, S., Raghavan, K. (2004). Importance of using physiologically relevant volume of dissolution medium to correlate the oral exposure of formulations of BMS-480188 mesylate. *Int. J. Pharm*., 269, 195–202.

25. Box, K., Comer, J. E., Gravestock, T., Stuart, M. (2009). New ideas about the solubility of drugs. *Chem. Biodivers*., 6, 1767–1788.

26. Ozaki, S., Minamisono, T., Yamashita, T., Kato, T., Kushida, I. (2011). Supersaturation-nucleation behavior of poorly soluble drugs and its impact on the oral absorption of drugs in thermodynamically high-energy forms. *J. Pharm. Sci*., 101(1), 214–22.

27. Kojima, T., Sugano, K., Onoue, S., Murase, N., Sato, M., Kawabata, Y., Mano, T. (2008). Solid form selection of zwitterionic 5-HT4 receptor agonist. *Int. J. Pharm*., 350, 35–42.

28. Tanaka, Y., Inkyo, M., Yumoto, R., Nagai, J., Takano, M., Nagata, S. (2009). Nanoparticulation of poorly water soluble drugs using a wet-mill process and physicochemical properties of the nanopowders. *Chem. Pharm. Bull. (Tokyo)*, 57, 1050–1057.
29. Takatsuka, T., Endo, T., Jianguo, Y., Yuminoki, K., Hashimoto, N. (2009). Nanosizing of poorly water soluble compounds using rotation/revolution mixer. *Chem. Pharm. Bull. (Tokyo)*, 57, 1061–1067.
30. Niwa, T., Miura, S., Danjo, K. (2011). Universal wet-milling technique to prepare oral nanosuspension focused on discovery and preclinical animal studies - development of particle design method. *Int. J. Pharm*., 405, 218–227.
31. Liversidge, G. G., Cundy, K. C. (1995). Particle size reduction for improvement of oral bioavailability of hydrophobic drugs: I. Absolute oral bioavailability of nanocrystalline danazol in beagle dogs. *Int. J. Pharm*., 125, 91–97.
32. Pouton, C. W. (2006). Formulation of poorly water-soluble drugs for oral administration: physicochemical and physiological issues and the lipid formulation classification system. *Eur. J. Pharm. Sci*., 29, 278–287.
33. MacGregor, K. J., Embleton, J. K., Lacy, J. E., Perry, E. A., Solomon, L. J., Seager, H., Pouton, C. W. (1997). Influence of lipolysis on drug absorption from the gastrointestinal tract. *Adv. Drug Delivery Rev*., 25, 33–46.
34. Dahan, A., Hoffman, A. (2007). The effect of different lipid based formulations on the oral absorption of lipophilic drugs: the ability of in vitro lipolysis and consecutive ex vivo intestinal permeability data to predict in vivo bioavailability in rats. *Eur. J. Pharm. Biopharm*., 67, 96–105.
35. Porter, C. J. H., Trevaskis, N. L., Charman, W. N. (2007). Lipids and lipid-based formulations: optimizing the oral delivery of lipophilic drugs. *Nat. Rev. Drug Discov*., 6, 231–248.
36. Trevaskis, N. L., Charman, W. N., Porter, C. J. (2008). Lipid-based delivery systems and intestinal lymphatic drug transport: a mechanistic update. *Adv. Drug Delivery Rev*., 60, 702–716.
37. Caliph, S. M., Charman, W. N., Porter, C. J. (2000). Effect of short-, medium-, and long-chain fatty acid-based vehicles on the absolute oral bioavailability and intestinal lymphatic transport of halofantrine and assessment of mass balance in lymph-cannulated and non-cannulated rats. *J. Pharm. Sci*., 89, 1073–1084.
38. Chiou, W. L., Riegelman, S. (1971). Pharmaceutical applications of solid dispersion systems. *J. Pharm. Sci*., 60, 1281–1302.
39. Serajuddin, A. T. (1999). Solid dispersion of poorly water-soluble drugs: early promises, subsequent problems, and recent breakthroughs. *J. Pharm. Sci*., 88, 1058–1066.
40. Friesen, D. T., Shanker, R., Crew, M., Smithey, D. T., Curatolo, W. J., Nightingale, J. A. (2008). Hydroxypropyl methylcellulose acetate succinate-based spray-dried dispersions: an overview. *Mol. Pharm*., 5, 1003–1019.
41. Gao, P., Rush, B. D., Pfund, W. P., Huang, T., Bauer, J. M., Morozowich, W., Kuo, M. S., Hageman, M. J. (2003). Development of a supersaturable SEDDS (S-SEDDS) formulation of paclitaxel with improved oral bioavailability. *J. Pharm. Sci*., 92, 2386–2398.
42. Gao, P., Guyton, M. E., Huang, T., Bauer, J. M., Stefanski, K. J., Lu, Q. (2004). Enhanced oral bioavailability of a poorly water soluble drug PNU-91325 by supersaturatable formulations. *Drug Dev. Ind. Pharm*., 30, 221–229.

43. Gao, P., Morozowich, W. (2006). Development of supersaturatable self-emulsifying drug delivery system formulations for improving the oral absorption of poorly soluble drugs. *Expert Opin. Drug Deliv*., 3, 97–110.

44. Brouwers, J., Brewster, M. E., Augustijns, P. (2009). Supersaturating drug delivery systems: the answer to solubility-limited oral bioavailability? *J. Pharm. Sci*., 98, 2549–2572.

45. Qian, K. K., Bogner, R. H. (2011). Application of mesoporous silicon dioxide and silicate in oral amorphous drug delivery systems. *J. Pharm. Sci*., 75(3), 354–365.

46. Van Speybroeck, M., Mols, R., Mellaerts, R., Thi, T. D., Martens, J. A., Van Humbeeck, J., Annaert, P., Van den Mooter, G., Augustijns, P. (2010). Combined use of ordered mesoporous silica and precipitation inhibitors for improved oral absorption of the poorly soluble weak base itraconazole. *Eur. J. Pharm. Biopharm*., 75, 354–365.

47. Van Speybroeck, M., Mellaerts, R., Mols, R., Thi, T. D., Martens, J. A., Van Humbeeck, J., Annaert, P., Van den Mooter, G., Augustijns, P. (2010). Enhanced absorption of the poorly soluble drug fenofibrate by tuning its release rate from ordered mesoporous silica. *Eur. J. Pharm. Sci*., 41, 623–630.

48. Mellaerts, R., Aerts, A., Caremans, T. P., Vermant, J., Van den Mooter, G., Martens, J. A., Augustijns, P. (2010). Growth of itraconazole nanofibers in supersaturated simulated intestinal fluid. *Mol. Pharm*., 7, 905–913.

49. Mellaerts, R., Mols, R., Kayaert, P., Annaert, P., Van Humbeeck, J., Van den Mooter, G., Martens, J. A., Augustijns, P. (2008). Ordered mesoporous silica induces pH-independent supersaturation of the basic low solubility compound itraconazole resulting in enhanced transepithelial transport. *Int. J. Pharm*., 357, 169–179.

50. Lindfors, L., Forssen, S., Westergren, J., Olsson, U. (2008). Nucleation and crystal growth in supersaturated solutions of a model drug. *J. Colloid Interface Sci*., 325, 404–413.

51. Varia, S. A., Schuller, S., Sloan, K. B., Stella, V. J. (1984). Phenytoin prodrugs III: water-soluble prodrugs for oral and/or parenteral use. *J. Pharm. Sci*., 73, 1068–1073.

52. Varia, S. A., Stella, V. J. (1984). Phenytoin prodrugs V: in vivo evaluation of some water-soluble phenytoin prodrugs in dogs. *J. Pharm. Sci*., 73, 1080–1087.

53. Yuan, H., Li, N., Lai, Y. (2009). Evaluation of in vitro models for screening alkaline phosphatase-mediated bioconversion of phosphate ester prodrugs. *Drug Metab. Dispos*., 37, 1443–1447.

54. Imai, T., Ohura, K. (2010). The role of intestinal carboxylesterase in the oral absorption of prodrugs. *Curr. Drug Metab*., 11, 793–805.

55. Sun, J., Dahan, A., Amidon, G. L. (2010). Enhancing the intestinal absorption of molecules containing the polar guanidino functionality: a double-targeted prodrug approach. *J. Med. Chem*., 53, 624–632.

56. Ohura, K., Sakamoto, H., Ninomiya, S., Imai, T. (2010). Development of a novel system for estimating human intestinal absorption using Caco-2 cells in the absence of esterase activity. *Drug Metab. Dispos*., 38, 323–331.

57. Ohura, K., Nozawa, T., Murakami, K., Imai, T. (2011). Evaluation of transport mechanism of prodrugs and parent drugs formed by intracellular metabolism in Caco-2 cells with modified carboxylesterase activity: temocapril as a model case. *J. Pharm. Sci*., 100, 3985–3994.

58. Mizuma, T. (2008). Pharmacokinetic strategy for designing orally effective prodrugs overcoming biological membrane barriers: proposal of kinetic classification and criteria for membrane-permeable prodrug-likeness. *Chem. Bioinform. J*., 8, 25–32.
59. Balimane, P. V., Tamai, I., Guo, A., Nakanishi, T., Kitada, H., Leibach, F. H., Tsuji, A., Sinko, P. J. (1998). Direct evidence for peptide transporter (PepT1)-mediated uptake of a nonpeptide prodrug, valacyclovir. *Biochem. Biophys. Res. Commun*., 250, 246–251.
60. Ma, K., Hu, Y., Smith, D. E. (2011). Peptide transporter 1 is responsible for intestinal uptake of the dipeptide glycylsarcosine: studies in everted jejunal rings from wild-type and Pept1 null mice. *J. Pharm. Sci*., 100, 767–774.
61. Omkvist, D. H., Trangbaek, D. J., Mildon, J., Paine, J. S., Brodin, B., Begtrup, M., Nielsen, C. U. (2011). Affinity and translocation relationships via hPEPT1 of H-X aa-Ser-OH dipeptides: evaluation of H-Phe-Ser-OH as a pro-moiety for ibuprofen and benzoic acid prodrugs. *Eur. J. Pharm. Biopharm*., 77, 327–331.
62. Rais, R., Fletcher, S., Polli, J. E. (2011). Synthesis and in vitro evaluation of gabapentin prodrugs that target the human apical sodium-dependent bile acid transporter (hASBT). *J. Pharm. Sci*., 100, 1184–1195.
63. Gupta, S. V., Gupta, D., Sun, J., Dahan, A., Tsume, Y., Hilfinger, J., Lee, K. D., Amidon, G. L. (2011). Enhancing the intestinal membrane permeability of zanamivir: a carrier mediated prodrug approach. *Mol. Pharm*., 8(6), 2358–2367.
64. Yan, Z., Sun, J., Chang, Y., Liu, Y., Fu, Q., Xu, Y., Sun, Y., Pu, X., Zhang, Y., Jing, Y., Yin, S., Zhu, M., Wang, Y., He, Z. (2011). Bifunctional peptidomimetic prodrugs of didanosine for improved intestinal permeability and enhanced acidic stability: synthesis, transepithelial transport, chemical stability and pharmacokinetics. *Mol. Pharm*., 8, 319–329.
65. Mizuma, T., Ohta, K., Hayashi, M., Awazu, S. (1992). Intestinal active absorption of sugar-conjugated compounds by glucose transport system: implication of improvement of poorly absorbable drugs. *Biochem. Pharmacol*., 43, 2037–2039.
66. Mizuma, T., Awazu, S. (1998). Intestinal Na+/glucose cotransporter-mediated transport of glucose conjugate formed from disaccharide conjugate. *Biochim. Biophys. Acta*, 1379, 1–6.
67. Mizuma, T., Nagamine, Y., Dobashi, A., Awazu, S. (1998). Factors that cause the beta-anomeric preference of Na+/glucose cotransporter for intestinal transport of monosaccharide conjugates. *Biochim. Biophys. Acta*, 1381, 340–346.
68. Liu, F., Merchant, H. A., Kulkarni, R. P., Alkademi, M., Basit, A. W. (2011). Evolution of a physiological pH 6.8 bicarbonate buffer system: application to the dissolution testing of enteric coated products. *Eur. J. Pharm. Biopharm*., 78, 151–157.
69. Fadda, H. M., Merchant, H. A., Arafat, B. T., Basit, A. W. (2009). Physiological bicarbonate buffers: stabilisation and use as dissolution media for modified release systems. *Int. J. Pharm*., 382, 56–60.
70. Siepmann, J., Gopferich, A. (2001). Mathematical modeling of bioerodible, polymeric drug delivery systems. *Adv. Drug Delivery Rev*., 48, 229–247.
71. Borgquist, P., Korner, A., Piculell, L., Larsson, A., Axelsson, A. (2006). A model for the drug release from a polymer matrix tablet–effects of swelling and dissolution. *J. Controlled Release*, 113, 216–225.
72. Kaunisto, E., Abrahmsen-Alami, S., Borgquist, P., Larsson, A., Nilsson, B., Axelsson, A. (2010). A mechanistic modelling approach to polymer dissolution using magnetic resonance microimaging. *J. Controlled Release*, 147, 232–241.

73. Jia, X., Williams, R. A. (2007). A hybrid mesoscale modelling approach to dissolution of granules and tablets. *Chem. Eng. Res. Des*., 85, 1027–1038.
74. Thombre, A. G. (2005). Assessment of the feasibility of oral controlled release in an exploratory development setting. *Drug Discov. Today*, 10, 1159–1166.
75. Pawar, V. K., Kansal, S., Garg, G., Awasthi, R., Singodia, D., Kulkarni, G. T. (2011). Gastroretentive dosage forms: a review with special emphasis on floating drug delivery systems. *Drug Deliv*., 18, 97–110.
76. Chen, C., Cowles, V. E., Hou, E. (2011). Pharmacokinetics of gabapentin in a novel gastric-retentive extended-release formulation: comparison with an immediate-release formulation and effect of dose escalation and food. *J. Clin. Pharmacol*., 51, 346–358.
77. Berner, B., Cowles, V. E. (2006). Case studies in swelling polymeric gastric retentive tablets. *Expert Opin. Drug deliv*., 3, 541–548.
78. Youan, B. B. (2004). Chronopharmaceutics: gimmick or clinically relevant approach to drug delivery? *J. Controlled Release*, 98, 337–353.
79. Gandhi, B. R., Mundada, A. S., Gandhi, P. P. (2011). Chronopharmaceutics: as a clinically relevant drug delivery system. *Drug Deliv*., 18, 1–18.
80. Van den Mooter, G. (2006). Colon drug delivery. *Expert Opin. Drug Deliv*., 3, 111–125.
81. Shah, N., Shah, T., Amin, A. (2011). Polysaccharides: a targeting strategy for colonic drug delivery. *Expert Opin. Drug Deliv*., 8, 779–796.

CHAPTER 12

FOOD EFFECT

"It is not just food. It is M&S food."

—Marks & Spencer TV ad.

The modeling and simulation (M&S) of the food effect on oral drug absorption is one of the key areas where biopharmaceutical modeling can be applied. It is preferable to design a compound and formulation that is less susceptible to the food effect. In addition to meals, fruit juice and alcohol also affect the oral absorption of a drug.

12.1 PHYSIOLOGICAL CHANGES CAUSED BY FOOD

The changes in physiological conditions by food intake have already been discussed in Chapter 6 and are only briefly described here. The bile acid concentration in the GI fluid increases from ca. 3 mM in the fasted state to ca. 15 mM in the fed state. The stomach pH is increased from 1.5 to 6 immediately after food intake and gradually decreases to the fasted pH in 1 h [1]. In the small intestine, pH in the fed state is about 6, which is slightly lower than that in the fasted state (pH 6.5). The stomach emptying time ($T_{1/2}$) increases from ca. 10 min in the fasted state to ca. 60 min in the fed state. Food intake increases the intestinal motility and intestinal and hepatic blood flows. Among these physiological changes, the increase of bile micelles is the most significant postprandial

Biopharmaceutics Modeling and Simulations: Theory, Practice, Methods, and Applications, First Edition. Kiyohiko Sugano.

change that affects the oral absorption of a drug. The development of a simulated intestinal fluid to mimic the postprandial state has been extensively investigated.

12.1.1 Food Component

Food components have a significant impact on the food effect. FDA recommends that food effect studies should be conducted using meal conditions that are expected to provide the greatest food effect. A high fat (~50% of total caloric content of the meal) and high calorie (~800–1000 kcal) meals is recommended as a test meal for food effect studies. This test meal should derive approximately 150, 250, and 500–600 kcal from protein, carbohydrate, and fat, respectively. An example test meal would be two eggs fried in butter, two strips of bacon, two slices of toast with butter, 4 oz of hash brown potatoes, and 8 oz of whole milk (Table 12.1) [2].

The contraction of the gallbladder is stimulated by a small amount of lipid ingested. Carbohydrates increase the motility of the intestinal tract but not the gallbladder contraction [3]. Typical viscosities of meals lie in the range of 10 to 100,000 cP. Marciani and coworkers utilized echo planar magnetic resonance imaging (MRI) in humans to monitor the changes in viscosity of meals and demonstrated significant and rapid reductions in viscosity with time due to dilution by the gastric fluids [4]. Figure 12.1 shows the effect of food component on the stomach pH [5]. Protein increased the gastric pH, whereas carbohydrate (Moducal) and lipid did not.

12.1.2 Fruit Juice Components

Recently, fruit juice–drug interaction has been extensively investigated. Grapefruit is known to affect the oral absorption of CYP3A4 and OATP substrates. Figure 12.2 shows the major flavonoids in the grapefruit juice. Table 12.2 shows

TABLE 12.1 Examples of Meals Used in Food Effect Studies

Standard Breakfast Meal[a]	Ensure Plus[b]
One English muffin with butter	Energy, kJ, 1263
One fried egg	Energy, kcal, 300
One slice of cheese	Carbohydrate, g, 40.4
One slice of Canadian bacon	Protein, g, 12.5
One serving of hash browned (fried shredded) potatoes	Total fat, g, 8.4
	Saturated fatty acids, g, 0.98
6 oz orange juice	Essential fatty acids, g, 2.9
8 oz whole milk	Dietary fiber, g, 0
Carbohydrate 73 g, 292 kcal, 1222 kJ, 45% of calories	Water, g, 155
Protein 29 g, 116 kcal, 485 kJ, 18% of calories	Minerals, vitamins
Fat 27 g, 240 kcal, 1004 kJ, 37% of calories	

[a] FDA office of generic drugs.
[b] Nutritive value per 200 ml.

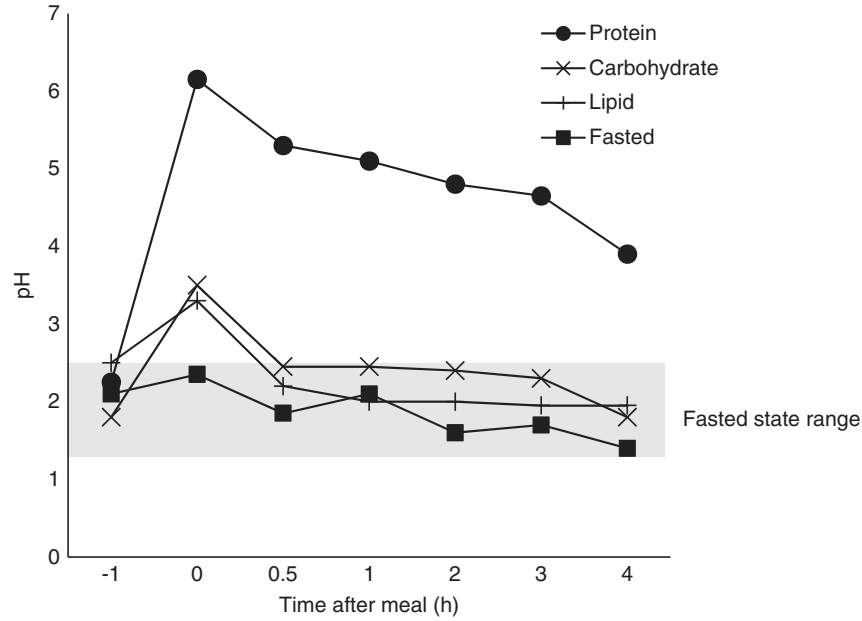

Figure 12.1 Stomach pH changes after meal administration. *Source:* Replotted from Reference 5.

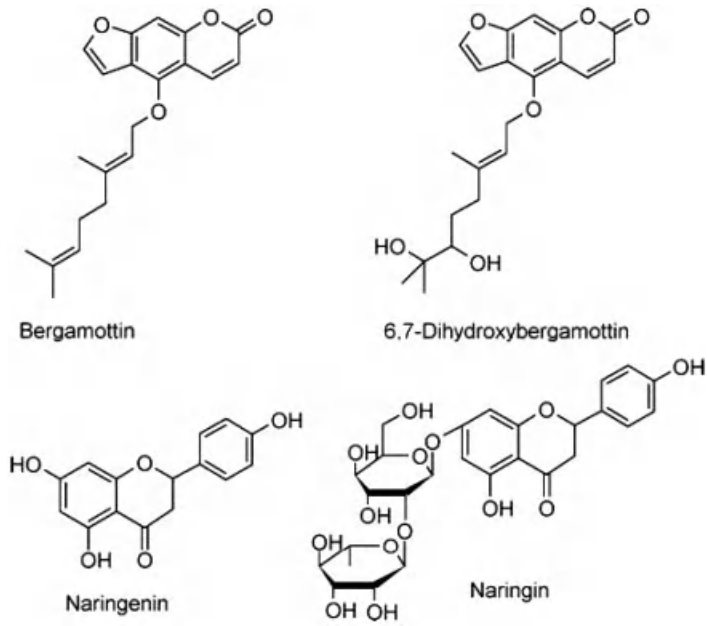

Figure 12.2 Structures of flavonoids and furanocoumarins present in grapefruit juice. *Source:* Adapted from Reference 8 with permission.

TABLE 12.2 Grapefruit Juice Component[a]

Type of Grapefruit Juice	Concentration, μM		
	Naringin	Bergamottin	6′,7′-Dihydroxybergamottin
Pink (3 brands)	782 ± 113	10.0 ± 2.9	0.6 ± 0.3
White (5 brands)	1010 ± 287	24.5 ± 7.6	14.5 ± 22.1
Red (6 brands)	473 ± 277	9.5 ± 6.3	5.6 ± 6.5

[a]References 6 and 8.

the typical concentration range of these flavonoids. The interaction via CYP3A is due to its high concentrations of DHB (6′,7′-dihydroxybergamottin) and/or the spiroester dimers, which are very potent irreversible inhibitors of enteric CYP3A [6]. Concentrated grapefruit juice was suggested to increase the GET, whereas normal grapefruit juice does not [7]. In addition, orange juice was suggested to decrease the oral absorption of OATP substrates (Section 12.2.3.2).

12.1.3 Alcohol

The concomitant intake of alcohol can cause an uncontrolled rapid release of a controlled-release formulation (dose dumping). Since a controlled-release formulation usually contains a larger drug amount than an IR formulation, if this amount is released at once, this could be a risk in clinical situations [9]. The FDA released drug-specific guidelines to test the effect of ethanol (5%, 20%, and 40% v/v) on the *in vitro* release profile of formulation (for tramadol, oxymorphone, morphine sulfate, bupropion, and metoprolol succinate) [10].

The alcohol intake delays the GET. Beer (500 ml), red wine (500 ml), and whiskey (125 ml) delayed the GET to 40, 70, and 25 min, respectively, compared to the control value of 15 min with 500 ml water [11].

In a prolonged-release formulation of hydromorphone, the C_{max} increased 1.9- and 5.5-fold when taken with 20% and 40% ethanol, respectively [12]. On the other hand, OROS [osmotic-controlled release oral delivery system (OROS^{TM})] formulation of the same drug was not susceptible to ethanol [13].

The effect of ethanol on intestinal membrane permeability is not well characterized [9]. Ethanol is metabolized mainly by the alcohol dehydrogenases and aldehyde dehydrogenases and to a minor extent by CYP2E1. About 99% of ethanol is metabolized in the liver [9].

12.2 TYPES OF FOOD EFFECTS AND RELEVANT PARAMETERS IN BIOPHARMACEUTICAL MODELING

12.2.1 Delay in T_{max} and Decrease in C_{max}

The delay in stomach emptying occurs, regardless of the drug property. However, the delay in T_{max} and reduction in C_{max} are often not observed for BCS II drugs,

as an increase in drug solubility in the intestine in the fed state masks these effects.

To investigate the appropriateness of the kinetic model for gastric emptying, biopharmaceutical modeling of acetaminophen was investigated, as shown in Figure 12.3 [14–16]. Acetaminophen is often used as a marker to investigate the GET. By setting the GET $T_{1/2}$ to 60 min, oral PK profile of acetaminophen in the fed state is appropriately reproduced (Fig. 12.3).

12.2.2 Positive Food Effect

A drug that shows a positive food effect usually has a dose number greater than 1 [18, 19] and high permeability (BCS II) [20, 21].

12.2.2.1 Bile Micelle Solubilization. Bile micelle solubilization has been suggested to be the major reason for a positive food effect for compounds with low solubility with Do > 1 (solubility-permeability-limited (SL) cases). However, this looks contradicting to the free fraction theory, as bile micelle solubilization would not increase the concentration of unbound drug (Section 2.3.3). This contradiction can be dispelled by considering the difference between the UWL- and epithelial-membrane-limited cases (SL-U and SL-E, respectively).

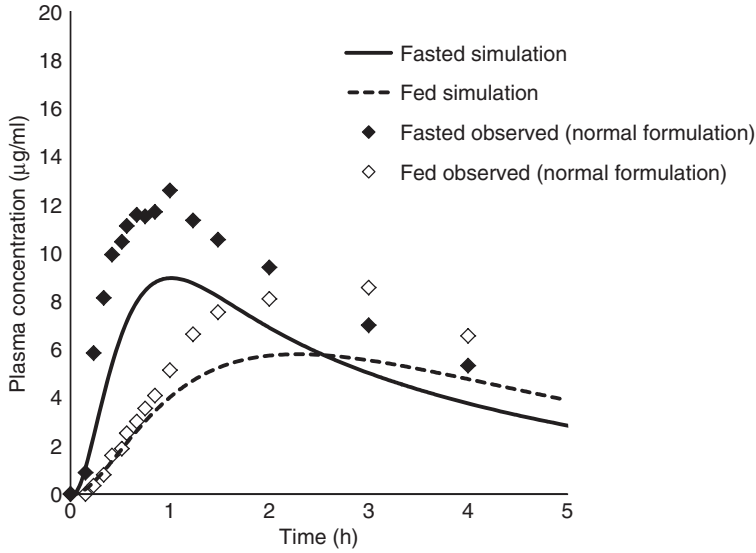

Figure 12.3 Food effect on acetaminophen PK. Dose = 1000 mg, $S_{\text{dissolv}} = 23.7$ mg/ml, $k_{\text{perm}} = 0.038$ min^{-1} (estimated from rat SPIP data [14], FgFh = 0.8 [14], $d_{\text{p}} = 1$ μm (immediate dissolution), $k_{12} = 0.95$ h^{-1}, $k_{21} = 1.41$ h^{-1}, $k_{13} = 0.51$ h^{-1}, and $V_1 = 0.6$ l/kg [17]. Gastric $T_{1/2} = 10$ min (fasted) and 60 min (fed). *Source:* Observed data from Reference 15.

The drug molecules bound to bile micelles can pass through the UWL. Once carried close to the epithelial membrane, the drug molecules, which are in rapid dynamic equilibrium between the bound and unbound states, then permeate the epithelial membrane. In the case of solubility-UWL-limited drugs (SL-U), the former process is slower than the latter process and becomes the rate-limiting step. Bile micelles increase the solubility of a drug ($S_{dissolv}$) (i.e., increase the dissolved drug concentration ($C_{dissolv}$)). At the same time, as the diffusion of bile-micelle-bound drug molecules is slower than that of unbound drug molecules, bile micelle binding reduces the effective diffusion coefficient (D_{eff}) of a drug in the UWL (Section 8.4.6). However, the D_{eff} does not become zero (cf. $D_{eff} = f_u \times D_{mono} + (1 - f_u) \times D_{bm}$). Consequently, the flux across the UWL is increased by bile micelle solubilization of a drug (cf. flux $= C_{dissolv} \times P_{UWL}$). For example, P_{UWL} of griseofulvin would be slightly decreased (0.6-fold), while its solubility is increased 2.3-fold, resulting in a net positive food effect (1.6-fold). Reduction in the effective permeability of griseofulvin by bile binding was experimentally observed [22].

Figure 12.4 shows the relationship between the lipophilicity of a drug and the clinical food effect for SL-U cases (undissociable drugs). A positive food effect

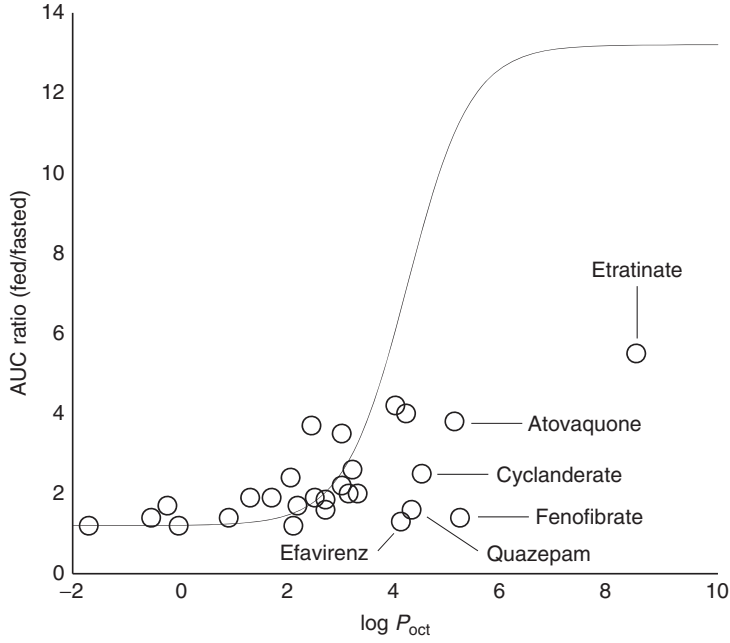

Figure 12.4 Relationship between lipophilicity of a drug and clinical food effect for SL-U cases (undissociable drugs). The solid line indicates an a priori theoretical line derived from log K_{bm} − log P_{oct} and log $P_{trans,0}$ − log P_{oct} relationships. D_{mono} and D_{bm} for the fasted and fed states were set to 7, 0.5, and 1.1×10^{-6} cm^2/s, respectively. V_{GI} ratio was set to 1.2.

by bile micelle solubilization would be observed for a compound with its log P_{oct} greater than 2. The theoretical line in Figure 12.4 shows an *a priori* prediction derived from the log K_{bm}–log P_{oct} equation (Eq. 2.17), the log $P_{trans,0}$–log P_{oct} equation (Eq. 4.34), and the diffusion coefficient of bile micelles. This theoretical line corresponds to the maximum food effect, so that when Fa% in the fed state is 100%, the fed/fasted AUC ratio can become less than the predicted values (Fig. 12.5). For example, if a drug has Fa% = 50% in the fasted state, the fed/fasted AUC ratio cannot exceed 2. Atovaquone (Fa% in the fasted state = 30%, the hereinafter the same), fenofibrate (51%), efavirenz (82%), cyclandelate (>40%), quazepam (>56%), and etretinate (30–70%) [23] would be such cases (Table 12.3). The positive food effect can be more than 10-fold, for example, halofantrine HCl (13-fold, 250 mg in dogs, log P_{oct} = 8.9) [24] and indomethacin farnesil (>50-fold, 150 mg in humans, calculated log P_{oct} = 9.6) [25]. The relationship between solubility ratio (FeSSIF/FaSSIF) and clinical food effect for SL-U cases is shown in Figure 12.5.

On the other hand, in the case of solubility–epithelial membrane limited drugs (SL-E), the oral absorption would not be increased by bile micelle solubilization. The bile-micelle-bound fraction cannot permeate across the epithelial cell membranes. Therefore, the flux through the epithelial membrane (the rate-limiting step) would not be increased (flux = $S_{dissolv} \times f_u P_{ep} = S_{blank}/f_u \times f_u P_{ep} = S_{blank} \times P_{ep}$). Pranlukast was suggested to be a typical example for this case (Tables 8.2 and 8.3). The solubility of pranlukast is increased ca. ninefold

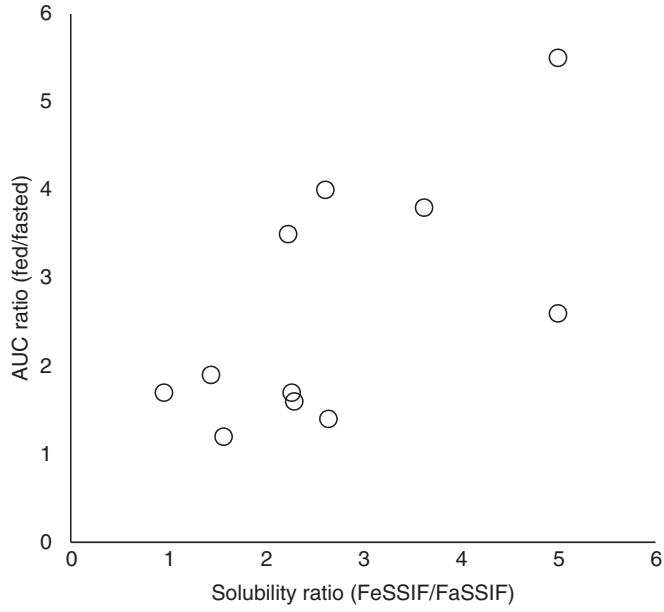

Figure 12.5 Relationship between solubility ratio (FeSSIF/FaSSIF) and clinical food effect for SL-U cases. (a) I.V. and (b) P.O.

TABLE 12.3 Food Effect for undissociable and Free Acid Drugs with Low Solubility[a]

				Solubility, mg/ml			References	
	$\log P_{oct}$	Dose, mg	Food Effect (Fed/Fasted)[b]	FaSSIF	FeSSIF	Solubility Ratio	Food Effect	Solubility
Indissociable								
Atovaquone	5.1	1000	3.8	0.0024	0.0087	3.6	19	26
Bropirimine	1.3[c]	500	1.9	—	—	—	19	—
Carbamazepine	2.1	400	1.2	0.185	0.29	1.6	18	27
Celecoxib	3	400	3.5	0.0462	0.103	2.2	28	29
Chlorothiazide	−0.24	500	1.7	0.87	0.83	0.95	18	26
Cyclandelate	4.49[c]	100	2.5	—	—	—	30	—
Danazol	4.2	100	4	0.018	0.047	2.6	19	26
Dicoumarol	2.7	250	1.85	—	—	—	18	—
Efavirenz	4.1	600	1.3	—	—	—	19	—
Etretinate	8.48	100	5.5	0.0034	0.017	5	18	31
Fenofibrate	5.2	200	1.4	0.014	0.037	2.6	—	32
FK-143	3	500	2.2	—	—	—	18	—
Ganciclovir	−1.7	1000	1.2	—	—	—	19	—
Griseofulvin	2.18	125	1.7	0.015	0.034	2.3	19	26
Hydrochloro-thiazide	−0.03	50	1.2	—	—	—	19	—
Ivermectin	3.2	30	2.6	0.12	0.6	5	33	26
Methoxsalen	1.7	1000	1.9	—	—	—	18	—
Lopinavir	2.3	400	1.7	—	—	—	—	—
Nitrofurantoin	−0.54	100	1.4	—	—	—	19	—
Phenytoin	2.5	350	1.9	0.041	0.059	1.4	18	26
Praziquantel	2.44[c]	1800	3.7	—	—	—	34	—
Proquazone	3.13	600	2	—	—	—	18	—
Quazepam	4.3	20	1.6	—	—	—	18	—
Repirinast	2.05[c]	300	2.4	—	—	—	18	—
Rufinamide	0.9	600	1.4	—	—	—	18	—
Spironolactone	3.3	200	2	—	—	—	18	—
Telaprevir	4	750	4.2	—	—	—	35	—
Troglitazone	2.7	400	1.6	0.0048	0.011	2.3	19	31
Free acid								
Acitretin	6.4	25	1.9	—	—	—	19	—
Isotretinoin	6	80	1.9	0.053	0.188	3.5	19	31
p-Aminosalicylic acid	1.6	6000	1.7	—	—	—	19	—
Pranlukast	4.2	225	1.3	0.088	0.8	9.1	19	26

[a] Compiled mainly from References 18, 19 for ≥ 1.2 cases.
[b] AUC ratio.
[c] Calculated by the ACD software.

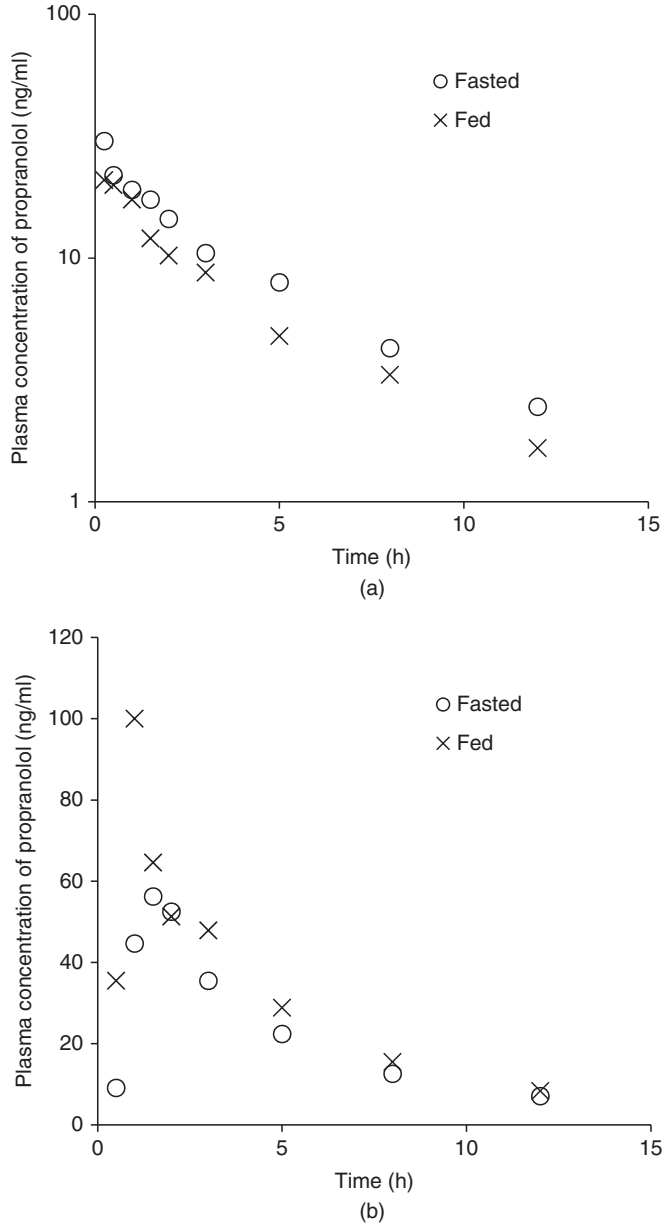

Figure 12.6 Plasma concentration-time curves for racemic propranolol after simultaneous dosing with 80-mg oral (p.o.) (b) and 0.1 mg/kg intravenous (i.v.) doses (a) (dotted line, fasted state; solid line, fed state). Mean ± SE; $n = 6$. *Source:* Adapted from Reference 41 with permission.

in the fed state. However, the food effect is only a 1.5-fold increase at 300 mg (cf. Fa% in the fed state is 11%). As the effective intestinal fluid volume would be increased after the food intake (estimated to be 1.2- to 1.5-fold), a slightly positive food effect can be observed for this class of drugs.

In the case of dissolution-rate-limited absorption, the bile micelle solubilization would increase the dissolution rate, leading to a positive food effect. For example, a positive food effect (2.6-fold) was observed in ivermectin (30-mg dose in humans) [36]. However, the increase in the dissolution rate by bile micelles is smaller than that of solubility as the effective diffusion coefficient is decreased [37].

A positive food effect is also observed for an oil formulation such as fenretinide (corn oil-polysorbate 80 [38], fed/fasted ratio = 3.2 [18]), pleconaril (MCT, 2.23) [39], and cyclosporine (emulsion, 3.8) [18].

In theory, the increase in the solubility of a drug by bile micelles may increase the drug concentration in the cytosol for SL-U cases, resulting in a decrease in the first-pass metabolism and the efflux transport. However, it is difficult to differentiate the contribution of increase in solubility, saturation of efflux transporter, and metabolism by inspecting the clinical PK data for such cases.

12.2.2.2 Increase in Hepatic Blood Flow. Fg is expressed as $Fg = 1 - CL_h/Q_h$. Therefore, the increase of the hepatic blood flow would reduce the hepatic first-pass effect and increase the bioavailability (Fig. 12.8). Drugs with CL_h of more than 6.5 ml/min/kg (32% of Q_h in humans) may exhibit a significant positive food effect [40]. Propranolol was suggested to be a typical example (Fig. 12.7) [41]. The BA% of propranolol (80-mg dose) was increased from 27% to 46% by food. Propranolol is mainly metabolized by CYP2D6, 1A2, and 2C19, suggesting that this positive food effect would not be Fg related [42]. Metoprolol [43], tolterodine [44], and propafenone [40] might be the other examples (1.4-, 1.5-, and 1.6-fold positive food effect, respectively; all metabolized mainly by CYP2D6). Rizatriptan might be another example (1.2-fold positive food effect [18], metabolized by monoamine oxidase) (Fig. 12.7; Table 12.4) [45].

12.2.2.3 Increase in Intestinal Blood Flow. Little or no positive food effect has been observed for atrovastatin [87], nisoldipine [88], and midazolam [89]. This evidence might suggest that intestinal blood flow has little effect on Fg [40].

Buspirone might be a case of positive food effect caused by the increase in the intestinal blood flow. Fg of buspirone is low (0.16) [90, 91]. AUC and C_{max} of unchanged buspirone increased by 84% and 116%, respectively, whereas the total amount of buspirone immunoreactive material did not change. This suggested that the presystemic metabolic clearance of buspirone was decreased by the food effect. As the dose number of buspirone is less than 0.5 (dose 20 mg, solubility >0.2 mg/ml), the solubility increase would not be the reason for the positive food effect. Deramciclane might be another example. AUC and C_{max} of unchanged deramciclane increased by 30% and 20%, respectively, whereas the total amount

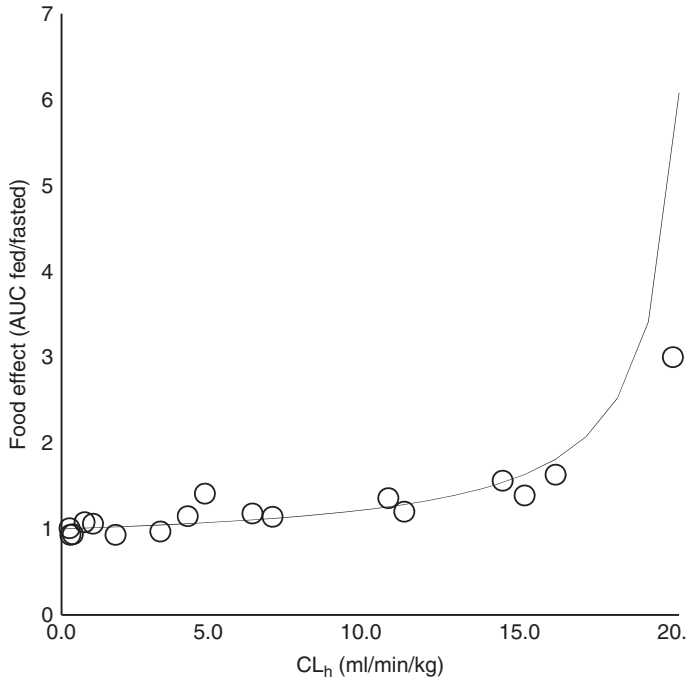

Figure 12.7 Hepatic clearance and food effect. The line indicates the theoretical prediction by $\mathrm{Fh} = 1 - CL_{\mathrm{h}}/Q_{\mathrm{h}}$.

of metabolite did not change [92]. Chloroquine and clarithromycin show positive food effects (1.4- and 1.2-fold, respectively) [18, 40], and CYP3A4 is involved in their metabolism. Fg of clarithromycin was estimated to be 0.87 from the grapefruit juice effect [93]. However, it is difficult to exclude the possibility of increase in Fh of these drugs. For drugs with low solubility and low Fg such as saquinavir, it is difficult to identify the main reason for the positive food effect.

12.2.2.4 Inhibition of Efflux Transporter and Gut Wall Metabolism. The components of grapefruit juice inhibit the CYP3A4 metabolism in the gut wall and significantly increase the exposure of a drug, which undergoes the gut wall metabolism. The inhibition of CYP3A4 by grapefruit juice occurs in the intestinal wall, but not in the liver [94]. Therefore, the grapefruit effect on bioavailability of a drug was suggested to be a good surrogate to estimate Fg [94]. The mean recovery half-life of intestinal CYP3A4 is 23 ± 10 h, which is shorter than that in hepatic CYP3A4 (1–6 d) [94].

To the best of the author's knowledge, little or no clinical evidence showing inhibition of P-gp by fruit juice has been reported [95]. With 220 ml single-strength grapefruit juice, digoxin AUC 0–24 was minimally increased to 1.1-fold, compared with water (not statistically significant) [96, 97]. *In vitro*, fruit juices moderately inhibited the P-gp effect [98].

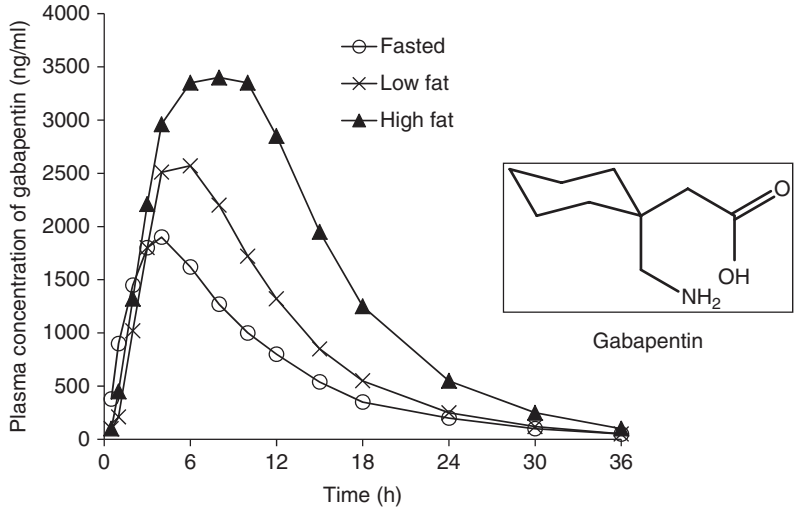

Figure 12.8 Effect of food and fat content on gabapentin C_p-time profiles following a single-dose oral administration of gabapentin (600 mg) as gastric retention extended-release formulation. The low fat meal contained 836 kcal, <30% of which was from fat. The high fat meal contained 945 kcal, of which approximately 50% was from fat. *Source:* Replotted from Reference 100.

TABLE 12.4 Positive Food Effect via Increase in Hepatic Blood Flow

	CL_h, ml/min/kg	Food Effect (Fed/Fasted)	References
Chloroquine	4.6	1.4	40
Diazepam	0.4	0.9	40
Diprafenone	10.6	1.4	40
Fluconazole	0.3	0.9	40
Labetalol	27.0	1.4	116
Metoprolol	15.0	1.4	40
Oxycodone	11.1	1.2	18
Pindolol	4.1	1.2	40
Prednisolone	1.0	1.1	40
Primaquine	6.8	1.1	40
Propafenone	14.3	1.6	40
Propranolol	16.0	1.6	40
Pyrazinamide	0.3	1.0	40
Quinidine	3.2	1.0	40
Selegiline	19.8	3	117
Stavudine	1.7	0.9	40
Theophylline	0.7	1.1	40
Timolol	6.2	1.2	40

Even though it has been theoretically suggested that the bile acids and food components can inhibit apical efflux transporters, little or no clinical evidence was reported.

In biopharmaceutical modeling, Fg estimation would be the key factor to estimate the effect of grapefruit juice on exposure of a drug (Section 4.10).

12.2.2.5 Desaturation of Influx Transporter. From the theoretical point of view, a slow gastric emptying can reduce the concentration of a drug in the upper intestine and increase the permeability of a drug via an uptake transporter. Together with the prolonged exposure of a drug to an upper-intestine-specific transporter, this could result in an increase in Fa%.

Gabapentin is absorbed via an L-amino acid transporter. This drug showed a dose-subproportional oral absorption. When dosed after a meal containing fat, the exposure of gabapentin was increased by 12% [99]. Interestingly, the food effect is more significant when dosed as a gastric retention formulation (Fig. 12.9) [100]. As this drug is very hydrophilic and zwitterionic, it is unlikely that pH and bile had affected its solubility in the intestine. Capsule and solution administration gave an identical oral absorption [99]. Therefore, the increase in exposure in the fed state would be due to the desaturation of uptake transport of gabapentin.

Ribavirin [101] and riboflavin [102] also show a positive food effect (both 1.4-fold). These compounds were also absorbed via influx transporters [103, 104].

12.2.3 Negative Food Effect

A drug that shows a negative food effect usually has a dose number less than 1 [18, 19] and low permeability (BCS III) [20, 21]. When compared to the positive food effects, the reasons for the negative food effects would be more complex. Two or more reasons may be acting simultaneously.

12.2.3.1 Bile Micelle Binding/Food Component Binding. Bile micelle binding has been suggested to be the reason for a negative food effect in drugs with low permeability and Do < 1 [22, 26, 31, 105–111]. Bile micelle binding reduces the unbound drug concentration at the epithelial surface and reduces the effective permeability of a drug (Fig. 12.9). In many low to moderately lipophilic base drugs, the food intake reduces the C_{max} and AUC. In spite of their hydrophilicity, nadolol and atenolol were found to bind to bile micelles and the effective intestinal permeability was reduced due to the reduction in the unbound fraction [112]. The extent of the negative food effect was found to quantitatively correlate with the free fraction ratio in FeSSIF/FaSSIF [31].

It is interesting that many compounds that show a negative food effect (Table 12.5) also show a bimodal PK profile [113], for example, pafenolol [108], talinolol [114] (Fig. 12.10), and maraviroc [115] (Fig. 12.11).[1] The second peak

[1]These drugs are also P-gp substrates and show dose-supralinear exposure (Section 14.2). A slower gastric emptying in the fed state may desaturate the efflux and decrease oral absorption of these drugs.

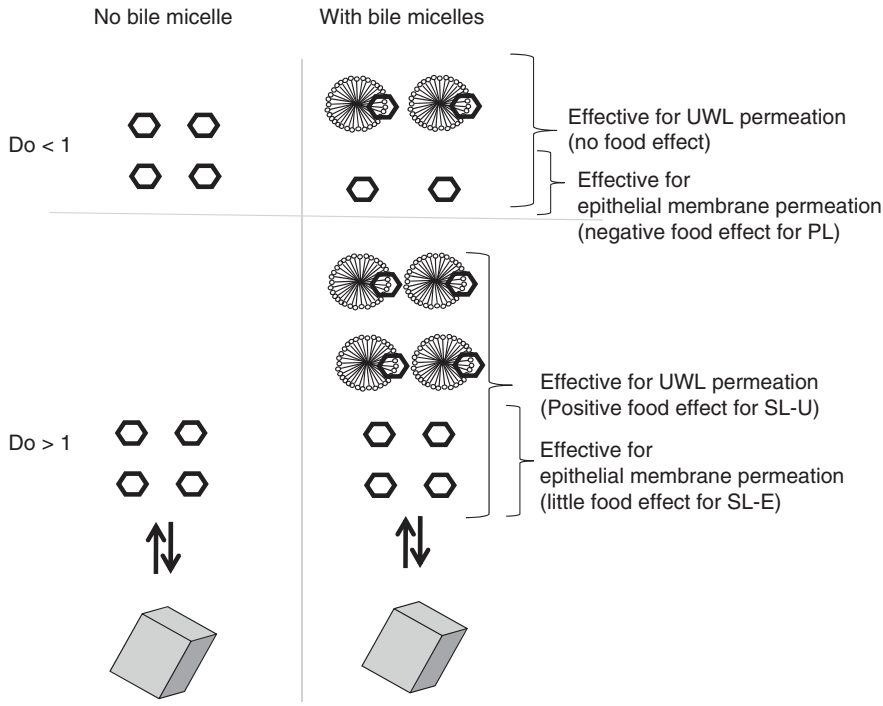

Figure 12.9 Concentration of free and bile-micelle-bound drug molecules in the presence and absence of undissolved solid drug. The bile-micelle-bound fraction is 50% for both Do > 1 and Do < 1 cases.

was found to be larger than the first peak, suggesting that the enterohepatic recirculation is not the reason for the bimodal PK profile. It was suggested that the drug molecules once bound to bile micelles in the upper small intestine would be released at the end of ileum as the bile acids are almost completely reabsorbed by a site-specific bile acid transporter (Fig. 12.12; Section 13.6.3.2) [108].

The oral absorption of bisphosphonates is significantly reduced when taken with food. Complex formation with Ca^{2+} would be the reason for this negative food effect.

12.2.3.2 Inhibition of Uptake Transporter. Fruit juice components can inhibit the uptake of a transporter substrate at the intestinal epithelial membrane. The oral absorptions of intestinal OATP substrates such as fexofenadine (Fig. 12.13) [118], celiprolol [119], talinolol [114], and aliskiren [120] are reduced when they are coadministered with grapefruit juice by 63%, 84%, 44%, and 61%, respectively. Inhibition of OATP uptake of these drugs by grapefruit components was suggested as the mechanism for clinical observation. It should be noted that orange juice is often taken in a food effect study (Table 12.1).

TABLE 12.5 Negative Food Effect

Drug	Food Effect[a]	Comments	References
5-Aminosalicylic acid	0.52	—	19
6-Thioguanine	0.41	—	18
Alendronate	<0.15	Bisphosphonate	129
Aliskiren	0.32	—	130
Ambenonium chloride	0.3	Quaternary amine	18
Amoxicillin	0.55	—	18
Aspirin	0.768	—	18
Atenolol	0.8	—	18
Bisamide	0.73	—	18
Bromazepam	0.67	—	18
Capecitabine	0.69	—	18
Captopril	0.44	—	18
Clodronate	0.7	Bisphosphonate	19
Didanosine	0.45	—	19
Delavirdine	0.74	—	65
Endralazine	0.33	—	131
Entecavir	0.79	—	19
Eptastigmine	0.63	—	19
Estramustine	0.674, 0.411	Alkylating agent	18
Etidronate	0	Bisphosphonate	132
Fenoldopam	0.35	Desaturation of metabolism	121
Fexofenadine	0.73[b]	—	133
Furosemide	0.55	—	19
Hydralazine	0.45	—	18
Indinavir sulfate	0.57	—	31
Isoniazid	0.57	—	19
Ketoprofen	0.78	—	18
Maraviroc	0.76	—	115
Melagatran	0.14	—	134
Melphalan	0.45	Alkylating agent	18
Metformin	0.76	—	18
Methotrexate	0.77	—	18
Nadolol	0.74	—	135
Nimodipine	0.62	—	18
Pafenolol	0.6	—	108
Penicillamine	0.49	—	18
Pidotimod	0.51	—	19
Pravastatin	0.69	—	19
Riluzole	0.8	—	31
Risedronate	0.44	Bisphosphonate	136
Sotalol	0.8	—	19
Sulpiride	0.71	—	18
Tacrine	0.79	—	18
Talinolol	0.5	—	137
Tamsulosin	0.7	—	19

(*continued*)

TABLE 12.5 (*Continued*)

Drug	Food Effect[a]	Comments	References
Tegaserod	0.45	—	138
Telmisartan	0.7	Solid dispersion formulation	139
Tetracycline	0.6	—	18
Tyramine	0.41	—	18
Voriconazole	0.56	—	125
Zafirlukast	0.78	Solubilized formulation	140
Zidovudine	0.67	—	18

[a] Compiled mainly from References 18, 19 for ≤ 0.8 cases.
[b] No orange juice included in the food study.

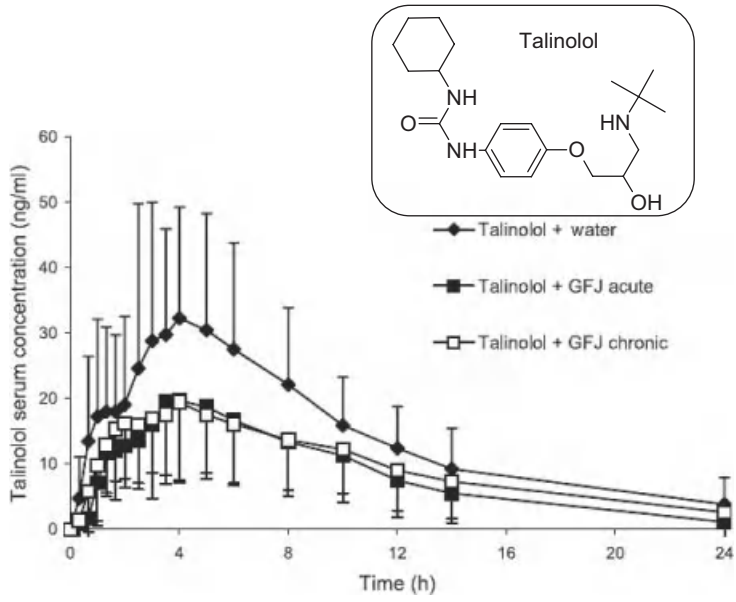

Figure 12.10 Mean (± SD) serum talinolol concentration–time profiles ($n = 24$) for orally administered talinolol (50 mg) with 300 ml of water, with 300 ml of grapefruit juice (GFJ acute), or after ingestion of 300 ml of grapefruit juice thrice daily for 6 d (GFJ chronic). *Source:* Adapted from Reference 114 with permission.

12.2.3.3 Desaturation of First-Pass Metabolism and Efflux Transport. Because of the slow stomach emptying, the dissolved drug concentration in the intestine in the fed state becomes lower than that in the fasted state, leading to desaturation of the first-pass metabolism (both at liver and gut wall) and the efflux transport in the intestine. Fenoldopam might be an example for this case [121]. The mean relative bioavailabilities (fed/fasted) were 35% and 81%, respectively, for fenoldopam and its sulfate metabolite (SK&F 87782) (Fig. 12.14).

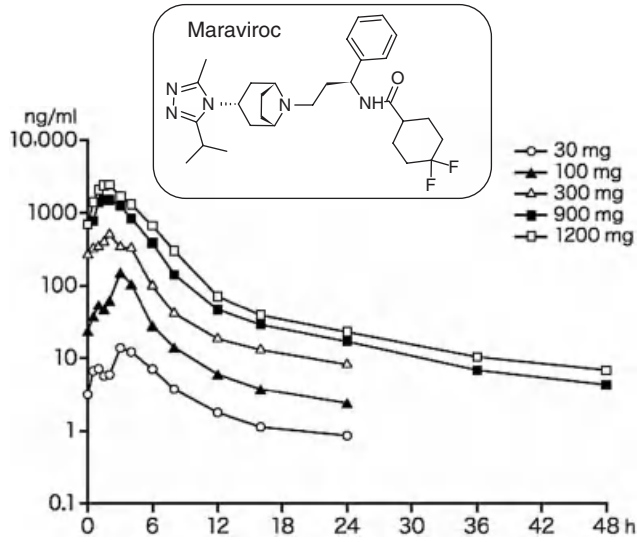

Figure 12.11 Mean plasma maraviroc concentration–time profiles after oral administration of maraviroc. *Source:* Adapted from Reference 115.

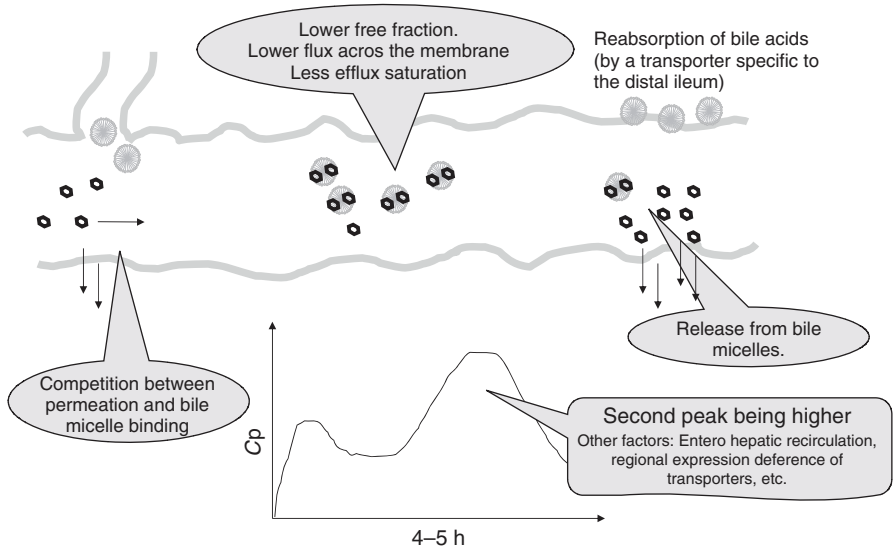

Figure 12.12 Bimodal PK and bile-micelle binding.

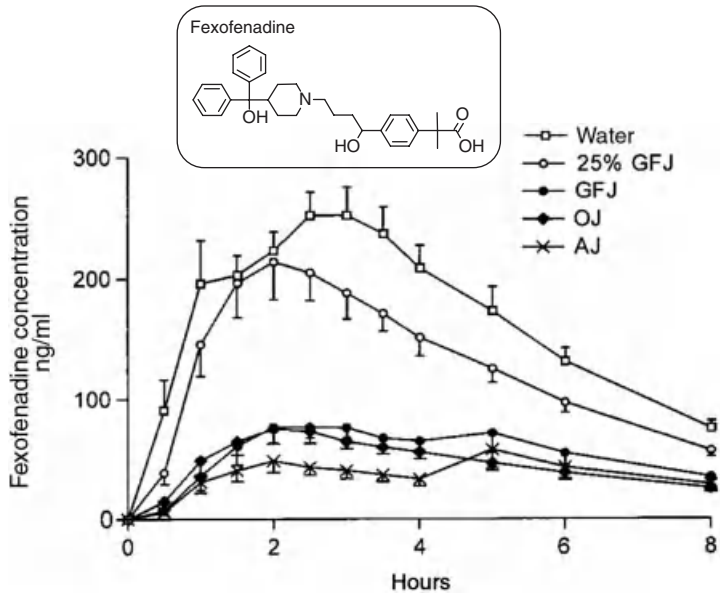

Figure 12.13 Mean plasma fexofenadine concentration-time profiles (n = 10) for orally administered fexofenadine (120 mg) with 300 ml water, grapefruit juice (GFJ) at 25% of regular strength (25% GFJ), GFJ, orange juice (OJ), or apple juice (AJ) followed by 150 ml of the same fluid every 0.5-3 h (total volume, 1.2 l). *Source:* Adapted from Reference 118 with permission.

Indinavir sulfate might be another example. The oral absorption of this drug was reduced by protein, carbohydrate, fat, and viscosity meal treatment (AUC ratio (fed/fasted) 32%, 55%, 67%, and 70%, respectively) [5]. The negative food effect by protein was considered to be due to the increased stomach pH. Oral absorption of indinavir sulfate is reduced by omeprazole, supporting this mechanism [122]. However, even though the meals containing carbohydrate and fat did not increase the stomach pH, they induced the negative food effects. Indinavir shows supraproportional exposure (40 vs 1000 mg) [123]. The negative food effect was reversed when a CYP3A4 inhibitor, ritonavir, was coadministered [86]. Grapefruit juice does not increase the bioavailability of indinavir, suggesting that intestinal metabolism is negligible [7]. Therefore, the slow gastric emptying and increased intestinal fluid volume in the fed state might have reduced the drug concentration in the portal vein and desaturated the liver first-pass metabolism. Delavirdine might also belong to this type of drugs, as it shows dose-supralinear exposure [63].

Voriconazole ($pK_a = 1.63$, $\log P_{oct} = 1.69$) [124] is an interesting example. In the fed state, the AUC of voriconazole after single dose of 200 mg is reduced to 57% of that in the fasted state. This negative food effect is less significant after multiple doses (78% at day 7) [125]. The bioavailability of voriconazole is 100% in the fasted state, and hence, there is no first-pass metabolism in the fasted state

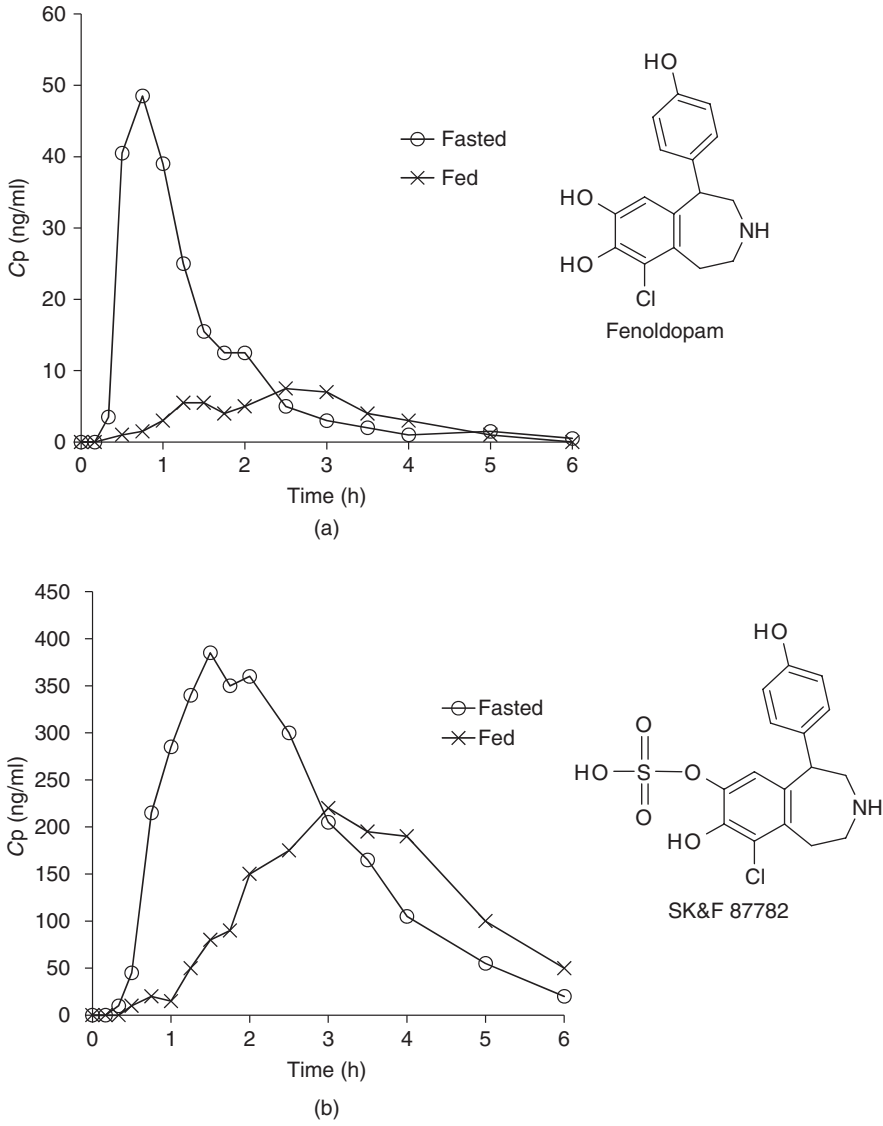

Figure 12.14 Mean plasma concentration (C_p)-time profile of (a) fenoldopam and (b) SK&F 87782 in humans in the fasted and fed states. *Source:* Replotted from Reference 121.

[124]. The solubility is similar in FaSSIF (0.66 mg/ml) and FeSSIF (0.73 mg/ml) (i.e., unbound fraction is similar), and the dose number is 1.2 (based on FaSSIF solubility and 200-mg dose) [31]. The gastric pH had no effect on oral absorption [126]. Therefore, the reduction of solubility in the stomach and permeability in the small intestine can be excluded from the possible mechanisms. Desaturation of

the first-pass metabolism would be one possible mechanism for the negative food effect. The AUC is dose-supralinear in 1.5–6.0 mg/kg after i.v. administration. Therefore, another possible mechanism for the negative food effect could be that as the C_{max} decreases due to slow gastric emptying, desaturation of systemic clearance (non-first-pass) occurred, leading to a decrease in AUC.

12.2.3.4 Viscosity. Food increases the viscosity of the chyme, and this can be a cause for a negative food effect. Solid meals caused a significant negative food effect on the oral absorption of bidisomide, whereas an equivalent caloric liquid food of relatively low viscosity did not. The negative meal effect on bidisomide was also generated by viscous zero-calorie meals [127]. The viscosity of chyme is greatest in the upper intestine where digestion of food is at its least complete. Therefore, viscosity is important when the drug is absorbed in the upper intestine. Food viscosity has been suggested to delay the disintegration of a paracetamol tablet [128].

12.2.3.5 pH Change in the Stomach. An increase in the stomach pH was speculated to be a reason for the negative food effect for base drugs with low solubility, as it would decrease the solubility and dissolution rate of a base drug in the stomach. However, little or no clinical evidence was reported to support this speculation. Actually, in contrast to the speculation, in the case of base drugs with low solubility, the food effect is usually positive (Table 12.6). A negative food effect is merely found for Do $>$ 1 cases [18, 19]. The increase in the solubility and the dissolution rate of a drug in the small intestine would cancel out the decrease in solubility in the stomach in the fed state.

12.2.3.6 pH Change in the Small Intestine. A decrease in the small intestinal pH was also speculated to be a reason for the negative food effect in a base drug with low permeability, as it would decrease the intestinal epithelial membrane permeability of the drug [21]. However, the microclimate pH is maintained relatively constant even when the bulk fluid pH was changed between pH 6.0 and 8.0 (Fig. 6.16). In addition, if this speculation was true, this pH effect should result in a positive food effect for acid drugs with low permeability. However, this is not clinically observed [18, 19]. On the contrary, acid drugs with low permeability usually show no or negative food effect (e.g., pravastatin, furosemide). As discussed earlier, the negative food effect observed for bases with low permeability can be explained by bile micelle binding. At present, little evidence exists to support a negative food effect via the intestinal pH change. Further investigation is required to prove this hypothesis.

12.3 EFFECT OF FOOD TYPE

It is well known that the positive food effect largely depends on the fat content of the food. The oral absorption of atovaquone in humans was higher when

TABLE 12.6 The Stomach pH and Food Effects for Dissociable Drugs with Low Solubility

Drug	pK_a	Fa% Change[a]		References	
		High/Low Gastric pH	Food Effect (Fed/Fasted)	Gastric pH	Food
Free base					
Albendazole	4.2	0.71 (1400 mg)	5	46	47
Aprepitant	4.2	—	1.31 (125 mg)	—	48
Cinnarizine	7.5	0.13–0.27 (25 mg)	1.2–1.7 (50 mg)	49	50
Clofazimine	8.5	0.85 (200 mg)	1.45 (200 mg)	51	51
Dasatinib	6.8	0.4 (50 mg)	1.2 (100 mg)	52	52
Dipyridamole	6.2	0.63	1	53	54
Gefitinib	5.28, 7.17	0.53 (250 mg)	1.37	55	55
Ketoconazole	2.9, 6.5	0.08 (200 mg)	0.61 (200 mg)[b] 1.05 (200 mg) 1.34 (200 mg)[d] 1.59 (400 mg)[c] 1.45 (600 mg)[c] 1.02 (800 mg)[c]	56	—
Itraconazole	3.7	0.35 (200 mg)[e] 0.54 (200 mg)[f]	3 (100 mg)	—	57
Posaconazole	3.6 4.6	0.66 (400 mg)	5 (400 mg)	58	58
Triclabendazole	3.1	—	3.7 (600 mg)	—	59
Salt of base					
Amiodarone HCl	9.0	—	2.4 (600 mg)	—	60
Atazanavir sulfate	4.25	0.25 (300 mg)	1.7 (400 mg)	61	62
Darunavir (ethanolate)	2.2	1 (400 mg)	1.4–1.8 (400 mg)	63	63
Dabigatran etexilate mesylate	4.0, 6.7	0.35 (200 mg)	1.42 (200 mg)	64	64
Delavirdine mesylate	4.6	0.52 (300 mg)	0.74 (300 mg)[g]	65	65
Erlotinib HCl	5.6	0.51 (150 mg)	2.9 (150 mg)	66	66
Halofantrine HCl	8.2	0.5 (250 mg in dogs)	3–5 (250–500 mg)[h] 13 (250 mg in dogs)[i]	67	—
Indinavir sulfate	3.8, 6.2	0.53 (800 mg)	0.57 (800 mg)[g,j] 0.88 (800 mg) (+RTV)[k]	68	—
Lapatinib tosylate	4.6, 6.7	—	4.25 (1500 mg)	—	69
Nelfinavir sulfate	6.0	0.36 (1250 mg)	2.4 (500 mg) 5.2 (1250 mg)	70	71

TABLE 12.6 (*Continued*)

Drug	pK_a	Fa% Change[a]		References	
		High/Low Gastric pH	Food Effect (Fed/Fasted)	Gastric pH	Food
Nilotinib HCl monohydrate	5.4	0.66 (400 mg)	1.8 (400 mg)	72	73
Saquinavir mesylate	7.0	—	6.7 (600 mg)	70, 74	75
Ticlopidine HCl	7.6	0.8 (250 mg)	1.2 (250 mg)	76	76
Ziprasidone HCl	6.5	—	2 (80 mg)	—	77
Salt of acid					
Raltegravir potassium	6.6	3.1 (400 mg)	Variable (Table 12.6)	78	79

[a] AUC ratio.
[b] Reference 80.
[c] Reference 81.
[d] Reference 56.
[e] Reference 82.
[f] Reference 83.
[g] Suggested to be due to desaturation of the hepatic first-pass effect.
[h] Reference 84.
[i] Reference 24.
[j] Reference 85.
[k] Reference 86.

TABLE 12.7 Effect of Food Type on Atovaquone (500-mg Tablet) Absorption in Humans[a]

	AUC, μgh/ml	C_{max}, μg/ml
Fasted	121 ± 74	1.5 ± 1.3
Two slices of toast	147 ± 144	1.7 ± 0.6
Two slices of toast + butter (23 g fat)	356 ± 165	5.7 ± 1.3
Two slices of toast + butter (56 g fat)	469 ± 152	8.3 ± 2.0
Fasted/CCK-OP (i.v.)	180 ± 47	1.7 ± 0.9

[a] Reference 141.

the fat content was higher (Table 12.7) [141]. To investigate the sole effect of endogenous bile micelles, cholecystokinin octapeptide (CCK-OP) was infused to induce gallbladder shrinkage. Compared to meals that are low and high in fat, CCK-OP had a smaller effect, suggesting that fat and/or digested fat affected the solubilization of atovaquone. This evidence support the advantage of FeSSIFv2 (which contains fatty acids and monoglycerides) compared to the original FeSSIF [142] as a surrogate for the real *in vivo* fluid in the fed state. The oral absorption of phenytoin in dogs (300 mg) was increased by casein and oleate (ca. 1.5- and

TABLE 12.8 Effect of Food Type on LY303366 (250 mg) Absorption in Dogs[a]

	AUC, μgh/ml	C_{max}, μg/ml
Fasted	21.2 ± 5.84	1.1 ± 0.27
Mixed meal (Ensure, 250 kcal)	8.9 ± 2.56	0.5 ± 0.17
Lipid meal (20% Intralipid, 250 kcal)	7.5 ± 1.84	0.4 ± 0.13
Protein meal (CASEC, 125 kcal)	8.9 ± 2.77	0.5 ± 0.20
Carbohydrate meal (Moducal, 125 kcal)	25.2 ± 5.13	1.6 ± 0.30

[a] Reference 144.

TABLE 12.9 Food Effect on Oral Absorption of Raltegravir Potassium (400 mg) in Humans[a]

	C_{max}, μM (90% CI)	AUC 0–12 (μM h) (90% CI)
Fasted	2.71 (1.80–4.08)	10.0 (7.20–14.0)
Low fat	1.31 (0.87–1.97)	5.38 (3.86–7.50)
Moderate fat	2.85 (1.89–4.29)	11.3 (8.12–15.8)
High fat	5.32 (3.53–8.01)	21.2 (15.2–29.6)

[a] Reference 79.

2-fold, respectively), but not by glucose and saline [143]. The positive food effect was reversed by coadministration of CCK antagonist. These results may suggest that the bile secretion is necessary, but not sufficient, for the positive food effect via increased solubility.

The extent of the negative food effect is also affected by the type of food. The oral absorption of LY303366 was reduced by lipid and protein meals, but not by carbohydrate meal (Table 12.8) [144]. Coadministration of CCK antagonist did not reverse the negative food effect.

Raltegravir is an interesting example [79]. With food low in fat, the food effect is negative, whereas with a meal high in fat, it is positive (Table 12.9).

12.4 BIOPHARMACEUTICAL MODELING OF FOOD EFFECT

12.4.1 Simple Flowchart and Semiquantitative Prediction

It is empirically well established that when the dose number (Do) of a drug is larger than 1, the food effect, when it occurs, would be positive [18, 19, 31]. In addition, the drugs with high lipophilicity also tend to show a positive food effect. These empirical classifications are theoretically supported by the GUT framework and would suggest that bile micelle binding/solubilization is the most frequent and significant reason for the positive food effect. The positive food effect is often observed for SL-U cases, sometimes as well as for DL cases.

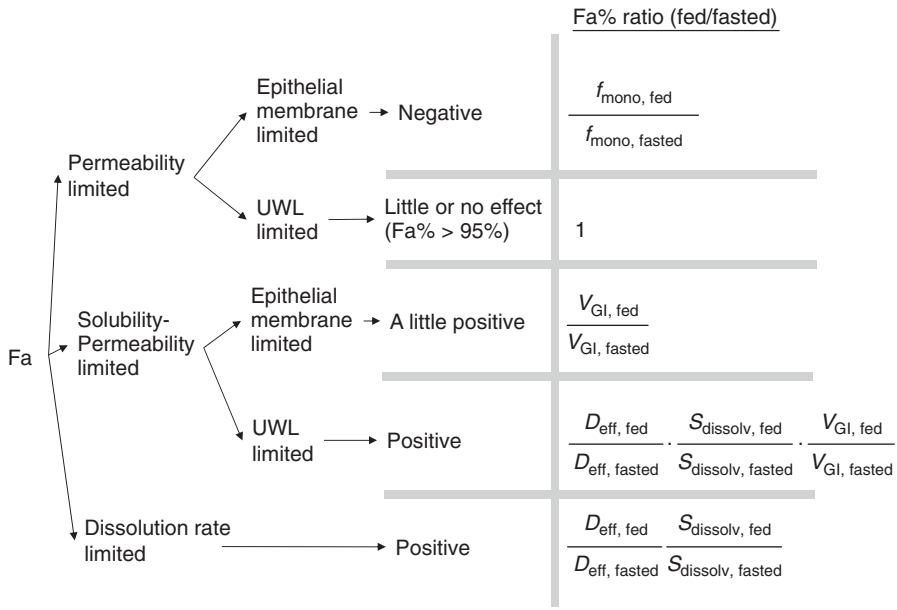

Figure 12.15 Mechanism-based flowchart to estimate the food effect by bile micelles.

On the other hand, for Do < 1 and drugs with low permeability, a negative food effect would be observed.[2] As discussed, based on the GUT framework, the food effect by bile micelles will be (Fig. 12.15)

- permeability-limited case: negative food effect
- dissolution-rate-limited case: positive food effect
- solubility–epithelial membrane permeability limited case: no or a little positive food effect
- solubility–UWL permeability limited case: positive food effect.

12.4.2 More Complicated Cases

Food intake simultaneously changes various physiological factors. Theoretically, biopharmaceutical modeling can handle this complicated situation. However, as the first step, we should first confirm that the effect of each physiological factor is well simulated by biopharmaceutical modeling. Prospective prediction of the food effects on intestinal metabolism and a carrier-mediated transport are challenging. As a prerequisite for this, the effect of these factors on Fa% in the fasted state should be well predicted. However, this has not been achieved yet (Chapter 14).

[2]Telmisartan [44] and zafirlukast [45] show negative food effect, although these compounds have low solubility, probably because these drugs are formulated using a solubilization technique.

Predictions for the effects of various meal types are also a challenging area. The first step will be characterizing the GI physiology after taking various types of meals.

Meanwhile, the applicable area of biopharmaceutical modeling will be limited to some simple factors such as bile micelles, GET, and gastric pH.

REFERENCES

1. Dressman, J. (1986). Comparison of canin and human gastrointestinal physiology. *Pharm. Res*., 3, 123–130.
2. Klein, S., Butler, J., Hempenstall, J.M., Reppas, C., Dressman, J.B. (2004). Media to simulate the postprandial stomach I. Matching the physicochemical characteristics of standard breakfasts. *J. Pharm. Pharmacol*., 56, 605–610.
3. Scholz, A., Abrahamsson, B., Diebold, S.M., Kostewicz, E., Polentarutti, B.I., Ungell, A.L., Dressman, J.B. (2002). Influence of hydrodynamics and particle size on the absorption of felodipine in labradors. *Pharm. Res*., 19, 42–46.
4. Mudie, D.M., Amidon, G.L., Amidon, G.E. (2010). Physiological parameters for oral delivery and in vitro testing. *Mol. Pharm*., 7, 1388–1405.
5. Carver, P.L., Fleisher, D., Zhou, S.Y., Kaul, D., Kazanjian, P., Li, C. (1999). Meal composition effects on the oral bioavailability of indinavir in HIV-infected patients. *Pharm. Res*., 16, 718–724.
6. Farkas, D., Greenblatt, D.J. (2008). Influence of fruit juices on drug disposition: discrepancies between in vitro and clinical studies. *Expert Opin. Drug Metab. Toxicol*., 4, 381–393.
7. Penzak, S.R., Acosta, E.P., Turner, M., Edwards, D.J., Hon, Y.Y., Desai, H.D., Jann, M.W. (2002). Effect of Seville orange juice and grapefruit juice on indinavir pharmacokinetics. *J. Clin. pharmacol*., 42, 1165–1170.
8. De Castro, W.V., Mertens-Talcott, S., Rubner, A., Butterweck, V., Derendorf, H. (2006). Variation of flavonoids and furanocoumarins in grapefruit juices: a potential source of variability in grapefruit juice-drug interaction studies. *J. Agric. Food. Chem*., 54, 249–255.
9. Lennernas, H. (2009). Ethanol-drug absorption interaction: potential for a significant effect on the plasma pharmacokinetics of ethanol vulnerable formulations. *Mol. Pharm*., 6, 1429–1440.
10. FDA, www.fda.gov/downloads/Drugs/GuidanceComplianceRegulatoryInformation/Guidances.
11. Franke, A., Teyssen, S., Harder, H., Singer, M.V. (2004). Effect of ethanol and some alcoholic beverages on gastric emptying in humans. *Scand. J. Gastroenterol*., 39, 638–644.
12. Walden, M., Nicholls, F.A., Smith, K.J., Tucker, G.T. (2007). The effect of ethanol on the release of opioids from oral prolonged-release preparations. *Drug Dev. Ind. Pharm*., 33, 1101–1111.
13. Sathyan, G., Sivakumar, K., Thipphawong, J. (2008). Pharmacokinetic profile of a 24-hour controlled-release OROS formulation of hydromorphone in the presence of alcohol. *Curr. Med. Res. Opin*., 24, 297–305.

14. Kalantzi, L., Reppas, C., Dressman, J.B., Amidon, G.L., Junginger, H.E., Midha, K.K., Shah, V.P., Stavchansky, S.A., Barends, D.M. (2006). Biowaiver monographs for immediate release solid oral dosage forms: acetaminophen (paracetamol). *J. Pharm. Sci*., 95, 4–14.

15. Rostami-Hodjegan, A., Shiran, M.R., Ayesh, R., Grattan, T.J., Burnett, I., Darby-Dowman, A., Tucker, G.T. (2002) A new rapidly absorbed paracetamol tablet containing sodium bicarbonate. I. A four-way crossover study to compare the concentration-time profile of paracetamol from the new paracetamol/sodium bicarbonate tablet and a conventional paracetamol tablet in fed and fasted volunteers. *Drug Dev. Ind. Pharm*., 28, 523–531.

16. Stillings, M., Havlik, I., Chetty, M., Clinton, C., Schall, R., Moodley, I., Muir, N., Little, S. (2000). Comparison of the pharmacokinetic profiles of soluble aspirin and solid paracetamol tablets in fed and fasted volunteers. *Curr. Med. Res. Opin*., 16, 115–124.

17. Rawlins, M.D., Henderson, D.B., Hijab, A.R. (1977). Pharmacokinetics of paracetamol (acetaminophen) after intravenous and oral administration. *Eur. J. Clin. pharmacol*., 11, 283–286.

18. Singh, B.N. (2005). A quantitative approach to probe the dependence and correlation of food-effect with aqueous solubility, dose/solubility ratio, and partition coefficient (Log P) for orally active drugs administered as immediate-release formulations. *Drug Dev. Res*., 65, 55–75.

19. Gu, C.H., Li, H., Levons, J., Lentz, K., Gandhi, R.B., Raghavan, K., Smith, R.L. (2007). Predicting effect of food on extent of drug absorption based on physicochemical properties. *Pharm. Res*., 24, 1118–1130.

20. Wu, C.Y., Benet, L.Z. (2005). Predicting drug disposition via application of BCS: transport/absorption/ elimination interplay and development of a biopharmaceutics drug disposition classification system. *Pharm. Res*., 22, 11–23.

21. Marasanapalle, V.P., Crison, J.R., Ma, J., Li, X., Jasti, B.R. (2009). Investigation of some factors contributing to negative food effects. *Biopharm. Drug Dispos*., 30, 71–80.

22. Poelma, F.G.J., Breaes, R., Tukker, J.J. (1990). Intestinal absorption of drugs. III. The influence of taurocholate on the disappearance kinetics of hydrophilic and lipophilic drugs from the small intestine of the rat. *Pharm. Res*., 7, 392–397.

23. Etiretinate. Interview form.

24. Humberstone, A.J., Porter, C.J., Charman, W.N. (1996). A physicochemical basis for the effect of food on the absolute oral bioavailability of halofantrine. *J. Pharm. Sci*., 85, 525–529.

25. Farnesil, I. Interview form.

26. Sugano, K., Kataoka, M., Mathews, C.C., Yamashita, S. (2010). Prediction of food effect by bile micelles on oral drug absorption considering free fraction in intestinal fluid. *Eur. J. Pharm. Sci*., 40, 118–124.

27. Schwebel, H.J., van Hoogevest, P., Leigh, M.L., Kuentz, M. (2011). The apparent solubilizing capacity of simulated intestinal fluids for poorly water-soluble drugs. *Pharm. Dev. Technol*., 16, 278–286.

28. Celecoxib. FDA approval document.

29. Shono, Y., Jantratid, E., Janssen, N., Kesisoglou, F., Mao, Y., Vertzoni, M., Reppas, C., Dressman, J.B. (2009). Prediction of food effects on the absorption of celecoxib based on biorelevant dissolution testing coupled with physiologically based pharmacokinetic modeling. *Eur. J. Pharm. Biopharm*., 73, 107–114.
30. Kaniwa, N., Ogata, H., Aoyagi, N., Ejima, A., Takahashi, T., Uezono, Y., Imazato, Y. (1991). Effect of food on the bioavailability of cyclandelate from commercial capsules. *Clin. Pharmacol. Ther*., 49, 641–647.
31. Kawai, Y., Fujii, Y., Tabata, F., Ito, J., Metsugi, Y., Kameda, A., Akimoto, K., Takahashi, M. (2011). Profiling and trend analysis of food effects on oral drug absorption considering micelle interaction and solubilization by bile micelles. *Drug Metab. Pharmacokinet*, 26, 180–191.
32. Buch, P., Langguth, P., Kataoka, M., Yamashita, S. (2009). IVIVC in oral absorption for fenofibrate immediate release tablets using a dissolution/permeation system. *J. Pharm. Sci*., 98, 2001–2009.
33. Guzzo, C.A., Furtek, C.I., Porras, A.G., Chen, C., Tipping, R., Clineschmidt, C.M., Sciberras, D.G., Hsieh, J.Y.K., Lasseter, K.C. (2002). Safety, tolerability, and pharmacokinetics of escalating high doses of ivermectin in healthy adult subjects. *J. Clin. Pharmacol*., 42, 1122–1133.
34. Castro, N., Medina, R., Sotelo, J., Jung, H. (2000). Bioavailability of praziquantel increases with concomitant administration of food. *Antimicrob. Agents Chemother*., 44, 2903–2904.
35. Telaprevir. FDA approval document.
36. Ivermectine, Interview form, in.
37. Okazaki, A., Mano, T., Sugano, K. (2008). Theoretical dissolution model of polydisperse drug particles in biorelevant media. *J. Pharm. Sci*., 97, 1843–1852.
38. Desai, K.G., Mallery, S.R., Holpuch, A.S., Schwendeman, S.P. (2011). Development and in vitro-in vivo evaluation of fenretinide-loaded oral mucoadhesive patches for site-specific chemoprevention of oral cancer. *Pharm. Res*., 28, 2599–2609.
39. Abdel-Rahman, S.M., Kearns, G.L. (1998). Single-dose pharmacokinetics of a pleconaril (VP63843) oral solution and effect of food. *Antimicrob. Agents Chemother*., 42, 2706–2709.
40. Marasanapalle, V.P., Boinpally, R.R., Zhu, H., Grill, A., Tang, F. (2011). Correlation between the systemic clearance of drugs and their food effects in humans. *Drug Dev. Ind. Pharm*., 37, 1311–1317.
41. Olanoff, L.S., Walle, T., Cowart, T.D., Walle, U.K., Oexmann, M.J., Conradi, E.C. (1986). Food effects on propranolol systemic and oral clearance: support for a blood flow hypothesis. *Clin. Pharmacol. Ther*., 40, 408–414.
42. Masubuchi, Y., Hosokawa, S., Horie, T., Suzuki, T., Ohmori, S., Kitada, M., Narimatsu, S. (1994). Cytochrome P450 isozymes involved in propranolol metabolism in human liver microsomes. The role of CYP2D6 as ring-hydroxylase and CYP1A2 as N-desisopropylase. *Drug Metab. Dispos*., 22, 909–915.
43. Melander, A., Danielson, K., Schersten, B., Wahlin, E. (1977). Enhancement of the bioavailability of propranolol and metoprolol by food. *Clin. Pharmacol. Ther*., 22, 108–112.
44. Olsson, B., Brynne, N., Johansson, C., Arnberg, H. (2001). Food increases the bioavailability of tolterodine but not effective exposure. *J. Clin. pharmacol*., 41, 298–304.

45. Rizatriptan. Label information.
46. Schipper, H.G., Koopmans, R.P., Nagy, J., Butter, J.J., Kager, P.A., Van Boxtel, C.J. (2000). Effect of dose increase or cimetidine co-administration on albendazole bioavailability. *Am. J. Trop. Med. Hyg*., 63, 270–273.
47. Albendazole. Interview form.
48. Aprepitant (2009). Aprepitant Interview form. ver. 3.
49. Ogata, H., Aoyagi, N., Kaniwa, N., Ejima, A., Sekine, N., Kitamura, M., Inoue, Y. (1986). Gastric acidity dependent bioavailability of cinnarizine from two commercial capsules in healthy volunteers. *Int. J. Pharm*., 29, 113–120.
50. Guangli, W., Shuhua, X., Changxiao, L. (1997). Effect of food on bioavailabil ity of cinnarizine capsules. *Chin. J. Clin. Pharmacol. Ther*., 2, 249–252.
51. Nix, D.E., Adam, R.D., Auclair, B., Krueger, T.S., Godo, P.G., Peloquin, C.A. (2004). Pharmacokinetics and relative bioavailability of clofazimine in relation to food, orange juice and antacid. *Tuberculosis (Edinb)*, 84, 365–373.
52. Dasatinib. FDA approval document.
53. Russell, T.L., Berardi, R.R., Barnett, J.L., O'Sullivan, T.L., Wagner, J.G., Dressman, J.B. (1994). pH-Related changes in the absorption of dipyridamole in the elderly. *Pharm. Res*., 11, 136–143.
54. Dipyridamole. Interview form.
55. Gefitinib (2009). Gefitinib Interview form. ver. 3.
56. Lelawongs, P., Barone, J.A., Colaizzi, J.L., Hsuan, A.T.M., Mechlinski, W., Legendre, R., Guarnieri, J. (1988). Effect of food and gastric acidity on absorption of orally administered ketoconazole. *Clin. Pharm*., 7, 228–235.
57. Itraconazole. Interview form.
58. Krishna, G., Moton, A., Ma, L., Medlock, M.M., McLeod, J. (2009). Pharmacokinetics and absorption of posaconazole oral suspension under various gastric conditions in healthy volunteers. *Antimicrob. Agents Chemother*., 53, 958–966.
59. Lecaillon, J.B., Godbillon, J., Campestrini, J., Naquira, C., Miranda, L., Pacheco, R., Mull, R., Poltera, A.A. (1998). Effect of food on the bioavailability of triclabendazole in patients with fascioliasis. *Br. J. Clin. Pharmacol*., 45, 601–604.
60. Meng, X., Mojaverian, P., Doedee, M., Lin, E., Weinryb, I., Chiang, S.T., Kowey, P.R. (2001). Bioavailability of amiodarone tablets administered with and without food in healthy subjects. *Am. J. Cardiol*., 87, 432–435.
61. Zhu, L., Persson, A., Mahnke, L., Eley, T., Li, T., Xu, X., Agarwala, S., Dragone, J., Bertz, R. (2011). Effect of low-dose omeprazole (20mg daily) on the pharmacokinetics of multiple-dose atazanavir with ritonavir in healthy subjects. *J. Clin. pharmacol*., 51, 368–377.
62. Atazanavir. Interview form.
63. Darunavir. Interview form.
64. Methanesulfonate, D.E. Approval document (Japan).
65. Delavirdine. Interview form.
66. Erlotinib. Interview form.
67. Ajayi, F.O., Brewer, T., Greenfield, R., Fleckenstein, L. (1999). Absolute bioavailability of halofantrine-HCl: effect of ranitidine and pentagastrin treatment. *Clin. Res. Regul. Aff*., 16, 13–28.

68. Tappouni, H.L., Rublein, J.C., Donovan, B.J., Hollowell, S.B., Tien, H.C., Min, S.S., Theodore, D., Rezk, N.L., Smith, P.C., Tallman, M.N., Raasch, R.H., Kashuba, A.D. (2008). Effect of omeprazole on the plasma concentrations of indinavir when administered alone and in combination with ritonavir. *Am. J. Health Syst. Pharm*., 65, 422–428.

69. Lapatinib. Approval document.

70. Falcon, R.W., Kakuda, T.N. (2008). Drug interactions between HIV protease inhibitors and acid-reducing agents. *Clin. Pharmacokinet*, 47, 75–89.

71. Nelfinavir. Interview form.

72. Yin, O.Q., Gallagher, N., Fischer, D., Demirhan, E., Zhou, W., Golor, G., Schran, H. (2010). Effect of the proton pump inhibitor esomeprazole on the oral absorption and pharmacokinetics of nilotinib. *J. Clin. pharmacol*., 50, 960–967.

73. Nilotinib. FDA approval document.

74. Winston, A., Back, D., Fletcher, C., Robinson, L., Unsworth, J., Tolowinska, I., Schutz, M., Pozniak, A.L., Gazzard, B., Boffito, M. (2006). Effect of omeprazole on the pharmacokinetics of saquinavir-500mg formulation with ritonavir in healthy male and female volunteers. *AIDS*, 20, 1401–1406.

75. Saquinavir. Interview form.

76. Shah, J., Fratis, A., Ellis, D., Murakami, S., Teitelbaum, P. (1990). Effect of food and antacid on absorption of orally administered ticlopidine hydrochloride. *J. Clin. Pharmacol*., 30, 733–736.

77. Miceli, J.J., Glue, P., Alderman, J., Wilner, K. (2007). The effect of food on the absorption of oral ziprasidone. *Psychopharmacol. Bull*., 40, 58–68.

78. Iwamoto, M., Wenning, L.A., Nguyen, B.Y., Teppler, H., Moreau, A.R., Rhodes, R.R., Hanley, W.D., Jin, B., Harvey, C.M., Breidinger, S.A., Azrolan, N., Farmer, H.F. Jr, Isaacs, R.D., Chodakewitz, J.A., Stone, J.A., Wagner, J.A. (2009). Effects of omeprazole on plasma levels of raltegravir. *Clin. Infect. Dis*., 48, 489–492.

79. Brainard, D.M., Friedman, E.J., Jin, B., Breidinger, S.A., Tillan, M.D., Wenning, L.A., Stone, J.A., Chodakewitz, J.A., Wagner, J.A., Iwamoto, M. (2011). Effect of low-, moderate-, and high-fat meals on raltegravir pharmacokinetics. *J. Clin. pharmacol*., 51, 422–427.

80. Mannisto, P.T., Mantyla, R., Nykanen, S., Lamminsivu, U., Ottoila, P. (1982). Impairing effect of food on ketoconazole absorption. *Antimicrob. Agents Chemother*., 21, 730–733.

81. Daneshmend, T.K., Warnock, D.W., Ene, M.D., Johnson, E.M., Potten, M.R., Richardson, M.D., Williamson, P.J. (1984). Influence of food on the pharmacokinetics of ketoconazole. *Antimicrob. Agents Chemother*., 25, 1–3.

82. Jaruratanasirikul, S., Sriwiriyajan, S. (1998). Effect of omeprazole on the pharmacokinetics of itraconazole. *Eur. J. Clin. pharmacol*., 54, 159–161.

83. Lange, D., Pavao, J.H., Wu, J., Klausner, M. (1997). Effect of a cola beverage on the bioavailability of itraconazole in the presence of H2 blockers. *J. Clin. pharmacol*., 37, 535–540.

84. Halofantrin. FDA label.

85. Indinavir. Interview form.

86. Aarnoutse, R.E., Wasmuth, J.C., Fatkenheuer, G., Schneider, K., Schmitz, K., de Boo, T.M., Reiss, P., Hekster, Y.A., Burger, D.M., Rockstroh, J.K. (2003). Administration of indinavir and low-dose ritonavir (800/100mg twice daily) with food reduces nephrotoxic peak plasma levels of indinavir. *Antivir. Ther*., 8, 309–314.

87. Lennernas, H. (2003). Clinical pharmacokinetics of atorvastatin. *Clin. Pharmacokinet*, 42, 1141–1160.

88. Form, I., Nisoldipine, in.

89. Bornemann, L.D., Crews, T., Chen, S.S., Twardak, S., Patel, I.H. (1986). Influence of food on midazolam absorption. *J. Clin. pharmacol*., 26, 55–59.

90. Gammans, R.E., Mayol, R.F., LaBudde, J.A. (1986). Metabolism and disposition of buspirone. *Am. J. Med*., 80, 41–51.

91. FDA, Buspirone Label, in.

92. Drabant, S., Nemes, K.B., Horvath, V., Tolokan, A., Grezal, G., Anttila, M., Gachalyi, B., Kanerva, H., Al-Behaisi, S., Horvai, G., Klebovich, I. (2004). Influence of food on the oral bioavailability of deramciclane from film-coated tablet in healthy male volunteers. *Eur. J. Pharm. Biopharm*., 58, 689–695.

93. Cheng, K.L., Nafziger, A.N., Peloquin, C.A., Amsden, G.W. (1998). Effect of grapefruit juice on clarithromycin pharmacokinetics. *Antimicrob. Agents Chemother*., 42, 927–929.

94. Gertz, M., Davis, J.D., Harrison, A., Houston, J.B., Galetin, A. (2008). Grapefruit juice-drug interaction studies as a method to assess the extent of intestinal availability: utility and limitations. *Curr. Drug Metab*., 9, 785–795.

95. Kirby, B.J., Unadkat, J.D. (2007). Grapefruit juice, a glass full of drug interactions? *Clin. Pharmacol. Ther*., 81, 631–633.

96. Becquemont, L., Verstuyft, C., Kerb, R., Brinkmann, U., Lebot, M., Jaillon, P., Funck-Brentano, C. (2001). Effect of grapefruit juice on digoxin pharmacokinetics in humans. *Clin. Pharmacol. Ther*., 70, 311–316.

97. Parker, R.B., Yates, C.R., Soberman, J.E., Laizure, S.C. (2003). Effects of grapefruit juice on intestinal P-glycoprotein: evaluation using digoxin in humans. *Pharmacotherapy*, 23, 979–987.

98. Xu, J., Go, M.L., Lim, L.Y. (2003). Modulation of digoxin transport across Caco-2 cell monolayers by citrus fruit juices: lime, lemon, grapefruit, and pummelo. *Pharm. Res*., 20, 169–176.

99. Bockbrader, N. (1995) Clinical pharmacokinetics of gabapentin. *Drugs Today*, 31, 613–619.

100. Chen, C., Cowles, V.E., Hou, E. (2011). Pharmacokinetics of gabapentin in a novel gastric-retentive extended-release formulation: comparison with an immediate-release formulation and effect of dose escalation and food. *J. Clin. pharmacol*., 51, 346–358.

101. Ribavirin. Interview form.

102. Levy, G., Jusko, W.J. (1966). Factors affecting the absorption of riboflavin in man. *J. Pharm. Sci*., 55, 285–289.

103. Patil, S.D., Ngo, L.Y., Glue, P., Unadkat, J.D. (1998). Intestinal absorption of ribavirin is preferentially mediated by the Na+-nucleoside purine (N1) transporter. *Pharm. Res*., 15, 950–952.

104. Fujimura, M., Yamamoto, S., Murata, T., Yasujima, T., Inoue, K., Ohta, K.Y., Yuasa, H. (2010). Functional characteristics of the human ortholog of riboflavin transporter 2 and riboflavin-responsive expression of its rat ortholog in the small intestine indicate its involvement in riboflavin absorption. *J. Nutr*., 140, 1722–1727.

105. Yamaguchi, T., Oida, T., Ikeda, C., Sekine, Y. (1986). Intestinal absorption of a b-adrenergic blocking agent nadolol. III. Nuclear magnetic resonance spectroscopic study on nadolol-sodium cholate micellar complex and intestinal absorption of nadolol derivatives in rats. *Chem. Pharm. Bull*., 34, 4259–4264.

106. Yamaguchi, T., Ikeda, C., Sekine, Y. (1986). Intestinal absorption of a b-adrenergic blocking agent nadolol. II. Mechanism of the inhibitory effect on the intestinal absorption of nadolol by sodium cholate in rats. *Chem. Pharm. Bull*., 34, 3836–3843.

107. Yamaguchi, T., Ikeda, C., Sekine, Y. (1986). Intestinal absorption of a b-adrenergic blocking agent nadolol. I. Comparison of absorption behavior of nadolol with those of other b-blocking agents in rats. *Chem. Pharm. Bull*., 34, 3362–3369.

108. Lennernaes, H., Regaardh, C.G. (1993). Evidence for an interaction between the b-blocker pafenolol and bile salts in the intestinal lumen of the rat leading to dose-dependent oral absorption and double peaks in the plasma concentration-time profile. *Pharm. Res*., 10, 879–883.

109. Ingels, F., Beck, B., Oth, M., Augustijns, P. (2004). Effect of simulated intestinal fluid on drug permeability estimation across Caco-2 monolayers. *Int. J. Pharmaceutics*, 274, 221–232.

110. Dongowski, G., Fritzsch, B., Giessler, J., Haertl, A., Kuhlmann, O., Neubert, R.H.H. (2005). The influence of bile salts and mixed micelles on the pharmacokinetics of quinine in rabbits. *Eur. J. Pharmaceutics Biopharm*., 60, 147–151.

111. Persson, E.M., Nordgren, A., Forsell, P., Knutson, L., Oehgren, C., Forssen, S., Lennernaes, H., Abrahamsson, B. (2008). Improved understanding of the effect of food on drug absorption and bioavailability for lipophilic compounds using an intestinal pig perfusion model. *Eur. J. Pharm. Sci*., 34, 22–29.

112. de Castro, B., Gameiro, P., Guimaraes, C., Lima, J.L., Reis, S. (2001). Partition coefficients of beta-blockers in bile salt/lecithin micelles as a tool to assess the role of mixed micelles in gastrointestinal absorption. *Biophys. Chem*., 90, 31–43.

113. Davies, N.M., Takemoto, J.K., Brocks, D.R., Yanez, J.A. (2010). Multiple peaking phenomena in pharmacokinetic disposition. *Clin. Pharmacokinet*, 49, 351–377.

114. Schwarz, U.I., Seemann, D., Oertel, R., Miehlke, S., Kuhlisch, E., Fromm, M.F., Kim, R.B., Bailey, D.G., Kirch, W. (2005). Grapefruit juice ingestion significantly reduces talinolol bioavailability. *Clin. Pharmacol. Ther*., 77, 291–301.

115. Maraviroc. Interview form.

116. Daneshmend, T.K., Roberts, C.J. (1982). The influence of food on the oral and intravenous pharmacokinetics of a high clearance drug: a study with labetalol. *Br. J. Clin. Pharmacol*., 14, 73–78.

117. Barrett, J.S., Rohatagi, S., DeWitt, K.E., Morales, R.J., DiSanto, A.R. (1996). The effect of dosing regimen and food on the bioavailability of the extensively metabolized, highly variable drug eldepryl((R)) (Selegiline Hydrochloride). *Am. J. Ther*., 3, 298–313.

118. Dresser, G.K., Bailey, D.G., Leake, B.F., Schwarz, U.I., Dawson, P.A., Freeman, D.J., Kim, R.B. (2002). Fruit juices inhibit organic anion transporting polypeptide-mediated drug uptake to decrease the oral availability of fexofenadine. *Clin. Pharmacol. Ther*., 71, 11–20.

119. Ieiri, I., Doi, Y., Maeda, K., Sasaki, T., Kimura, M., Hirota, T., Chiyoda, T., Miyagawa, M., Irie, S., Iwasaki, K., Sugiyama, Y. (2011). Microdosing clinical study: pharmacokinetic, pharmacogenomic (SLCO2B1), and interaction (Grapefruit Juice) profiles of celiprolol following the oral microdose and therapeutic dose. *J. Clin. pharmacol*., [Epub ahead of print]

120. Tapaninen, T., Neuvonen, P.J., Niemi, M. (2010). Grapefruit juice greatly reduces the plasma concentrations of the OATP2B1 and CYP3A4 substrate aliskiren. *Clin. Pharmacol. Ther*., 88, 339–342.

121. Clancy, A., Locke-Haydon, J., Cregeen, R.J., Ireson, M., Ziemniak, J. (1987). Effect of concomitant food intake on absorption kinetics of fenoldopam (SK&F 82526) in healthy volunteers. *Eur. J. Clin. pharmacol*., 32, 103–106.

122. Beique, L., Giguere, P., la Porte, C., Angel, J. (2007). Interactions between protease inhibitors and acid-reducing agents: a systematic review. *HIV Med*., 8, 335–345.

123. Yeh, K.C., Deutsch, P.J., Haddix, H., Hesney, M., Hoagland, V., Ju, W.D., Justice, S.J., Osborne, B., Sterrett, A.T., Stone, J.A., Woolf, E., Waldman, S. (1998). Single-dose pharmacokinetics of indinavir and the effect of food. *Antimicrob. Agents Chemother*., 42, 332–338.

124. Voriconazole. Interview form.

125. Purkins, L., Wood, N., Kleinermans, D., Greenhalgh, K., Nichols, D. (2003) Effect of food on the pharmacokinetics of multiple-dose oral voriconazole. *Br. J. Clin. Pharmacol*., 56(Suppl 1), 17–23.

126. Purkins, L., Wood, N., Kleinermans, D., Nichols, D. (2003) Histamine H2-receptor antagonists have no clinically significant effect on the steady-state pharmacokinetics of voriconazole. *Br. J. Clin. Pharmacol*., 56(Suppl 1), 51–55.

127. Pao, L.H., Zhou, S.Y., Cook, C., Kararli, T., Kirchhoff, C., Truelove, J., Karim, A., Fleisher, D. (1998). Reduced systemic availability of an antiarrhythmic drug, bidisomide, with meal co-administration: relationship with region-dependent intestinal absorption. *Pharm. Res*., 15, 221–227.

128. Parojcic, J., Vasiljevic, D., Ibric, S., Djuric, Z. (2008). Tablet disintegration and drug dissolution in viscous media: paracetamol IR tablets. *Int. J. Pharm*., 355, 93–99.

129. Gertz, B.J., Holland, S.D., Kline, W.F., Matuszewski, B.K., Freeman, A., Quan, H., Lasseter, K.C., Mucklow, J.C., Porras, A.G. (1995). Studies of the oral bioavailability of alendronate. *Clin. Pharmacol. Ther*., 58, 288–298.

130. Aliskiren. Interview form.

131. Kindler, J., Ruegg, P.C., Neuray, M., Pacha, W. (1987). Effect of food intake on plasma levels and antihypertensive response during maintenance therapy with endralazine. *Eur. J. Clin. pharmacol*., 32, 367–372.

132. Etidronate. Interview form.

133. Stoltz, M., Arumugham, T., Lippert, C., Yu, D., Bhargava, V., Eller, M., Weir, S. (1997). Effect of food on the bioavailability of fexofenadine hydrochloride (MDL 16455A). *Biopharm. Drug Dispos*., 18, 645–648.

134. Eriksson, U.G., Bredberg, U., Hoffmann, K.J., Thuresson, A., Gabrielsson, M., Ericsson, H., Ahnoff, M., Gislen, K., Fager, G., Gustafsson, D. (2003). Absorption, distribution, metabolism, and excretion of ximelagatran, an oral direct thrombin inhibitor, in rats, dogs, and humans. *Drug Metab. Dispos*., 31, 294–305.

135. Buice, R.G., Subramanian, V.S., Duchin, K.L., Uko-Nne, S. (1996). Bioequivalence of a highly variable drug: an experience with nadolol. *Pharm. Res*., 13, 1109–1115.

136. Mitchell, D.Y., Heise, M.A., Pallone, K.A., Clay, M.E., Nesbitt, J.D., Russell, D.A., Melson, C.W. (1999). The effect of dosing regimen on the pharmacokinetics of risedronate. *Br. J. Clin. Pharmacol*., 48, 536–542.

137. Terhaag, B., Palm, U., Sahre, H., Richter, K., Oertel, R. (1992). Interaction of talinolol and sulfasalazine in the human gastrointestinal tract. *Eur. J. Clin. pharmacol*., 42, 461–462.

138. Zhou, H., Khalilieh, S., Lau, H., Guerret, M., Osborne, S., Alladina, L., Laurent, A.L., McLeod, J.F. (1999). Effect of meal timing not critical for the pharmacokinetics of tegaserod (HTF 919). *J. Clin. pharmacol*., 39, 911–919.

139. Telmisartan. Interview form.

140. Zafirlukast. Interview form.

141. Rolan, P.E., Mercer, A.J., Weatherley, B.C., Holdich, T., Meire, H., Peck, R.W., Ridout, G., Posner, J. (1994). Examination of some factors responsible for a food-induced increase in absorption of atovaquone. *Br. J. Clin. Pharmacol*., 37, 13–20.

142. Jantratid, E., Janssen, N., Reppas, C., Dressman, J.B. (2008). Dissolution media simulating conditions in the proximal human gastrointestinal tract: an update. *Pharm. Res*., 25, 1663–1676.

143. Miles, C., Dickson, P., Rana, K., Lippert, C., Fleisher, D. (1997). CCK antagonist pre-treatment inhibits meal-enhanced drug absorption in dogs. *Regul. Pept*., 68, 9–14.

144. Li, C., Fleisher, D., Li, L., Schwier, J.R., Sweetana, S.A., Vasudevan, V., Zornes, L.L., Pao, L.H., Zhou, S.Y., Stratford, R.E. (2001). Regional-dependent intestinal absorption and meal composition effects on systemic availability of LY303366, a lipopeptide antifungal agent, in dogs. *J. Pharm. Sci*., 90, 47–57.